LIQUID CRYSTAL MAPPING OF THE SURFACE TEMPERATURE ON A HEATED CYLINDER PLACED IN A CROSSFLOW OF AIR

Richard Johns Field

NAVAL POSTGRADUATE SCHOOL

Monterey, California

THESIS

LIQUID CRYSTAL MAPPING OF THE SURFACE
TEMPERATURE ON A HEATED CYLINDER
PLACED IN A CROSSFLOW OF AIR

by

Richard Johns Field

Thesis Advisor: T. E. Cooper

March 1974

Approved for public release; distribution unlimited.

Liquid Crystal Mapping of the Surface Temperature on a Heated Cylinder Placed in a Crossflow of Air

by

Richard Johns Field
Lieutenant, United States Navy
B.S., United States Naval Academy, 1967

Submitted in partial fulfillment of the
requirements for the degree of

MASTER OF SCIENCE IN MECHANICAL ENGINEERING

from the

NAVAL POSTGRADUATE SCHOOL
March 1974

ABSTRACT

A liquid crystal thermographic technique has been developed which provides an excellent means of obtaining both qualitative and quantitative heat transfer information on heated objects placed in forced convection environments.

Circumferential variation of the Nusselt number on a uniformly heated right circular cylinder cooled by forced convection was obtained for Reynolds numbers varying from 38,000 to 148,000. The results compare within the experimental uncertainty in forward stagnation regions with the theory of Schuh. Beyond approximately 30°, the results diverge from theory but are consistent with the work of other investigators.

TABLE OF CONTENTS

LIST OF TABLES

TABLE

LIST OF ILLUSTRATIONS

Figure

ACKNOWLEDGEMENT

I would like to thank Prof. Thomas Cooper for his interest and guidance during this project.

I. INTRODUCTION

The purpose of this investigation was to develop a technique for the visual determination of both qualitative and quantitative heat transfer and fluid flow information on heated objects placed in forced convection environments. Cholesteric liquid crystals, a material that exhibits brilliant changes in color over discrete, reproducible temperature bands, were used as the temperature sensor in the technique. The liquid crystals allow one to visually observe select isotherms and, further, can be used to infer the location of points of flow separation and boundary layer reattachment. The liquid crystals also give a dramatic indication of the influence of turbulence on surface temperature.

The technique has been used to determine the circumferential variation of the Nusselt number on a uniformly heated right circular cylinder cooled by forced convection in a cross flow of air. Reynolds numbers were varied from 38,000 to 148,000 in the present investigation. This allowed the study of both critical and subcritical flows. The free stream turbulence intensity was approximately 0.5 - 0.7%.

Data were obtained on a 4 inch diameter right circular cylinder constructed from .039 inch thick carbon impregnated paper that had a resistivity of approximately 1 ohm-in. The surface of the cylinder was electrically heated by passing a known current longitudinally through the paper. The inner hollow space formed by the cylinder was firmly packed with

glass wool to prevent heat losses into the cylinder. The glass wool also reinforced the cylinder and aided in resisting deformation due to the outer flow.

The results obtained in the present investigation compared within the estimated experimental uncertainty in the forward stagnation region with a theory proposed by Schuh [1]. Beyond approximately 30°, the experimental values rapidly diverge from the theory. This is consistent with results found by other investigators [2,3] and is most probably explained by the fact that the pressure distribution used in Schuh's theory was taken to be the ideal, frictionless distribution.

II. BACKGROUND

The use of liquid crystals in wind tunnel experiments was first investigated by Klein [4] in 1968. Although they showed great promise for obtaining heat transfer rates, several problems existed. The degree of accuracy was limited by the influences of mechanical shear, ultraviolet light, and chemical contamination.

Some time after the completion of Klein's study, the National Cash Register Company (NCR) developed a process for encapsulating liquid crystals. McElderry [5] used these crystals in a study of boundary layer transition at supersonic speeds, and found the encapsulated crystals to be relatively insensitive to shear and contamination.

Wirzburger [6], in a thesis study, used liquid crystals to study the heat transfer characteristics of a container stored rocket motor placed in a hostile environment. The temperature distributions produced by resistively heated, cryogenic, and radio-frequency surgical probes were studied by Groff, Petrovic, and Katz [7,8,9,10,11, 12] using liquid crystals.

One of the original objectives of a thesis investigation by Meyer [3] was to use encapsulated liquid crystals to study the surface temperature distribution on a uniformly heated cylinder cooled by a cross flow of air. This objective was never accomplished. The temperature distributions in his study were all found using thermocouples. The present investigation is a continuation of the work initiated by Meyer.

III. EXPERIMENTAL APPARATUS

A. LIQUID CRYSTALS

There are three types of liquid crystals; smectic, nematic, and cholesteric [13]. Of these three, only the cholesteric type was used in the present investigation.

Microencapsulated liquid crystals provide a visual display of temperature when applied to a black surface. The liquid crystal surface color will pass through the visible color spectrum in sequential order as a function of surface temperature. The temperature at which a given color appears is a function of the cholesterol ester formulation. By selecting the proper formulation the entire spectrum (red to

violet) can be transversed in fraction or multiple degrees with an accuracy of approximately 0.1°C [14]. Fergason [13, 15-17], in a series of articles, presents excellent discussions on the chemistry, varieties, properties, uses, and limitations of liquid crystals.

The process of microencapsulation consistsof enclosing the liquid crystals in 20-30 micron polyvinyl alcohol capsules. These capsules are suspended in a water based slurry. This process makes the liquid crystals relatively insensitive to mechanical shear and chemical contamination. It also reduces the sensitivity to viewing angle when compared to raw liquid crystals [5].

Fourteen different liquid crystal temperature formulations were used in the present study. A temperature range of 30°C to 49°C was covered. The liquid crystals used and their calibration points are listed in Table I.

The liquid crystals were calibrated using a Rosemount constant temperature bath following the general procedure outlined by Petrovic [8].

All crystals were calibrated on a piece of the material to which they would be applied for data collection. With the exception of liquid crystal R-45 all liquid crystals in Table I were calibrated on a piece of the carbon impregnated paper. A piece of tape was the base material for the R-45 calibration.

Table I

Liquid Crystal Calibration Results

Liquid Crystal (NCR Designation)	Color Transition Red(°F)	Green(°F)	Blue(°F)
S-30	85.9	86.4	87.5
S-32	90.5	91.6	92.6
R-33	92.8	93.7	95.6
S-34	94.4	95.2	96.3
S-36	97.5	98.2	99.4
R-37	98.9	99.7	102.4
S-38	101.4	102.4	103.4
S-40	105.1	106.1	107.1
R-41	106.1	107.4	109.8
S-43	109.8	111.0	112.3
S-45	113.2	114.0	115.1
R-45	108.9	109.9	121.1
R-49	121.7	122.0	124.2

B. CYLINDER DESIGNS AND CONSTRUCTION

The basic experimental procedure was first developed using the cylinder constructed for Meyer's work [3]. An improved procedure was established using a cylinder constructed from carbon impregnated paper. Final data were collected on a redesigned paper cylinder.

1. Meyer's Cylinder

The following is a brief description of Meyer's cylinder. A detailed description is contained in reference 3. The cylinder is shown in Figure 1. It was constructed of acrylic tubing with an outer diameter of 4.47 inches. The cylinder was 32 inches long and spanned the wind tunnel test section from roof to floor.

A surface heat flux was generated by energizing the 0.375 inch wide, 0.003 inch thick, Nichrome ribbon which was helically wrapped over the middle 15 1/8 inches. Guard heater circuits prevented end losses and a Silastic, RTV foam, limited internal convective losses.

Temperature information was obtained using thermocouples welded to the inner surface of the Nichrome ribbon. Two pressure taps were provided for obtaining surface pressure distributions. The cylinder was mounted on a turntable that could be rotated from outside the wind tunnel. This allowed temperature and pressure information to be obtained at all angular locations.

In the present set of experiments the cylinder was installed in the low speed Aerolab wind tunnel, located in

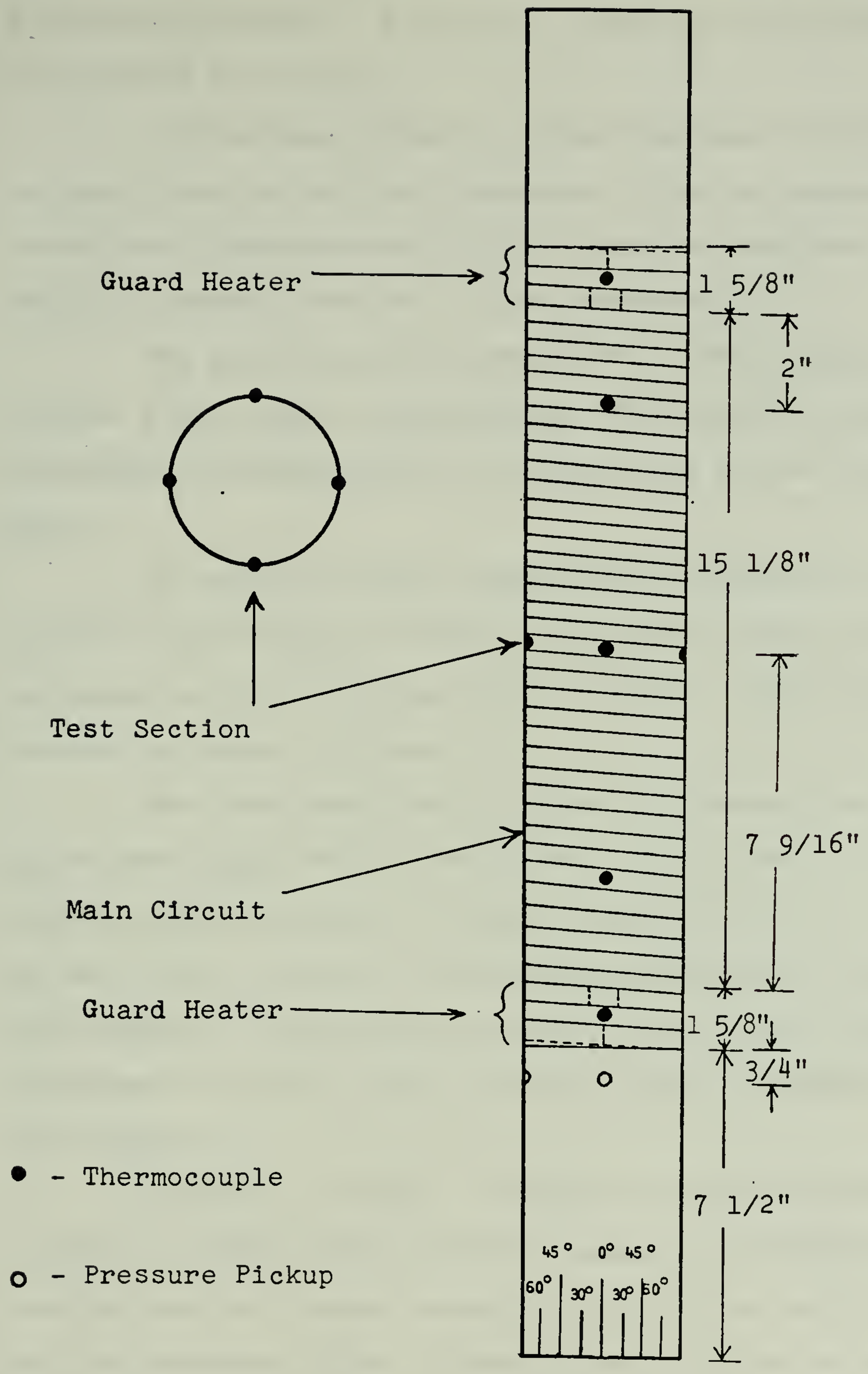

Figure 1 Meyer's Test Cylinder

the Aeronautics Laboratory in Halligan Hall, U.S. Naval Postgraduate School. A schematic diagram of the wind tunnel is provided in Figure 2.

The turbulence level of the wind tunnel was measured by Meyer using a hot wire anemometer. The turbulence level ranged from approximately 0.5% to 0.7% for the range of Reynolds numbers studied in this experiment.

The wind tunnel is powered by a 100hp electric motor, and has a four speed transmission. The tunnel is capable of achieving a maximum speed of 200 mph with a clear test section.

In order to obtain temperature information on Meyer's cylinder using liquid crystal, the crystals were first applied to tapes and the tapes were then applied to the cylinder surface as shown in Figure 3.

The tapes were made by spraying Testors flat black paint onto Scotch double coated tape number 404. A diluted liquid crystal solution was then applied with a paint brush in two coats. Finally, the entire assembly was sealed with Polyurethane. The process produced tapes with an approximate thickness of 0.009 in. and a crystal layer of approximately .004 inches.

As noted by Meyer, the surface of this cylinder had numerous surface irregularities caused by the difference in coefficients of thermal expansion between the acrylic tubing and the Nichrome ribbon. These irregularities can be seen in Figure 3, and were the primary reason for designing a new cylinder for continuing the investigation.

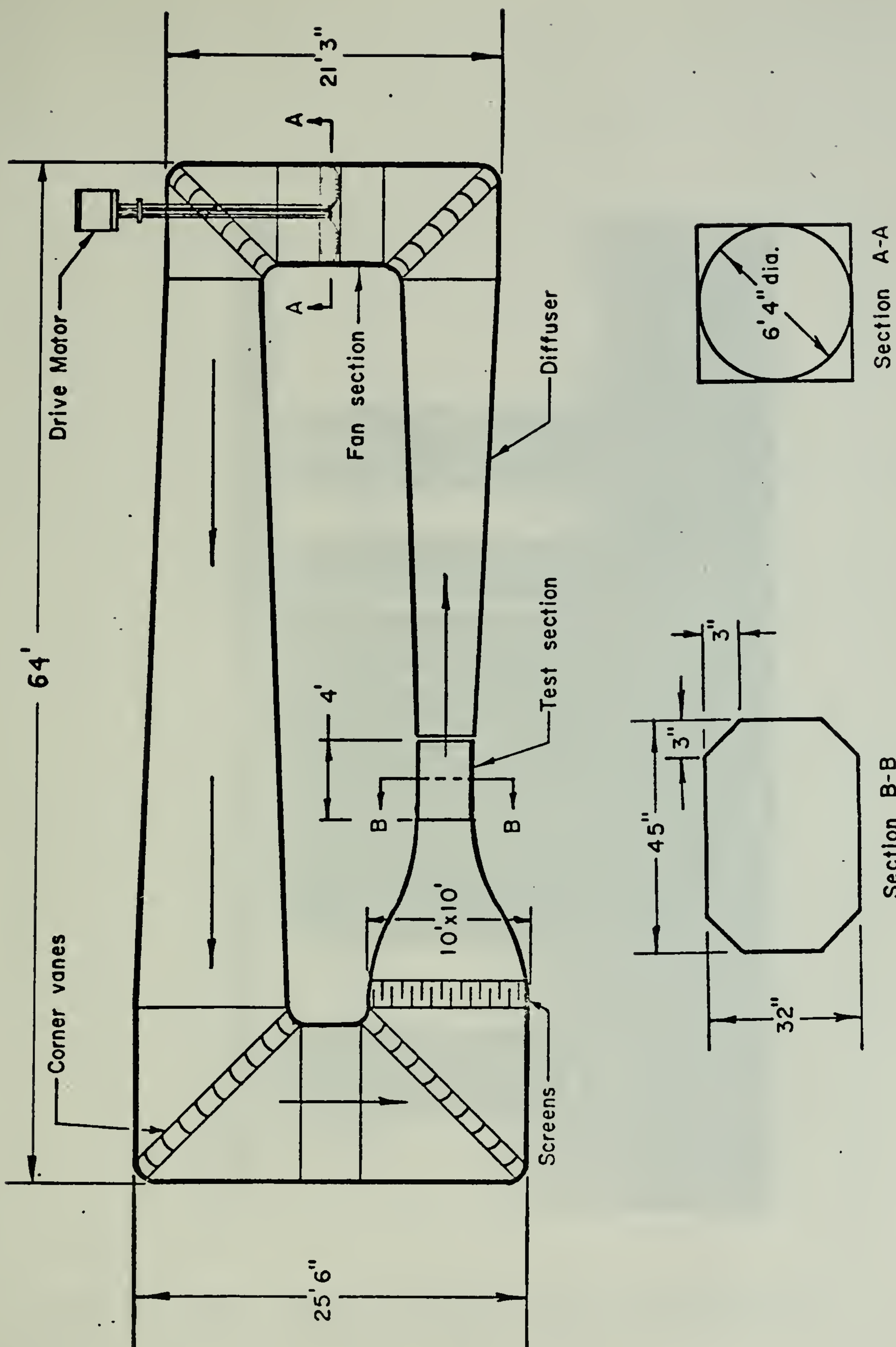

Figure 2 Schematic Diagram of the Wind Tunnel

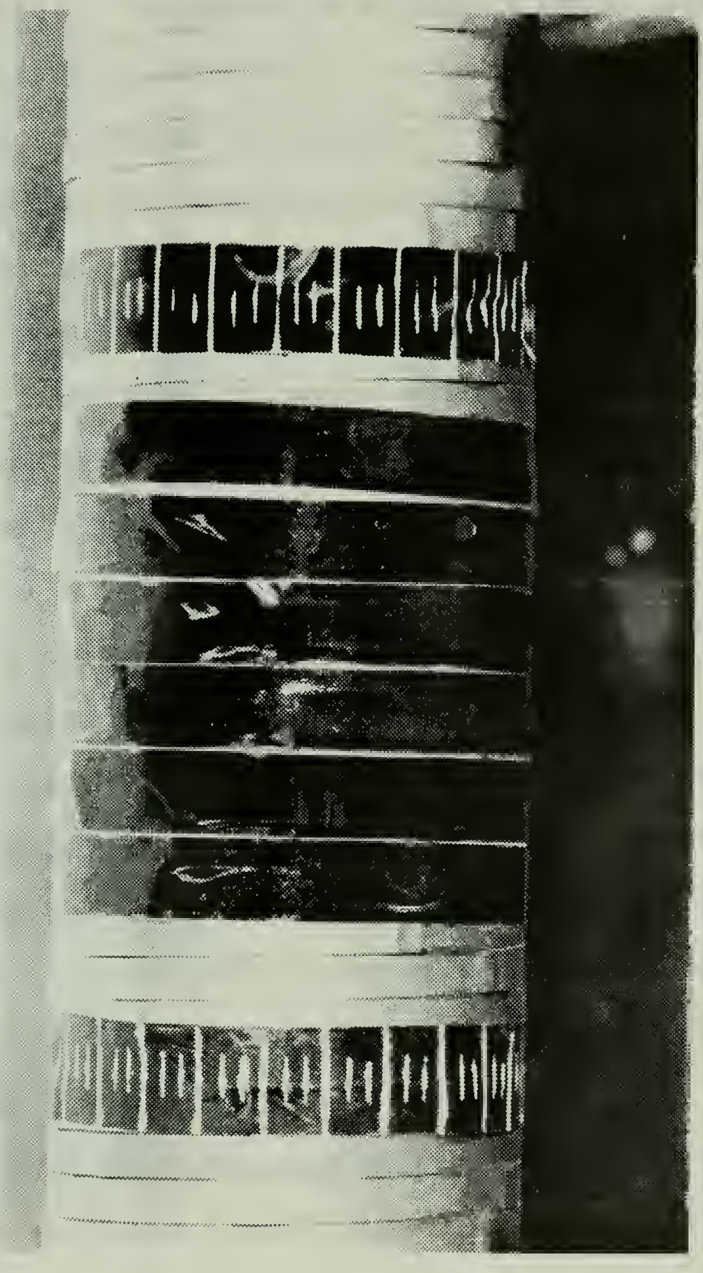

Figure 3. Test Cylinder with Surface Irregularities and the Liquid Crystal Tapes.

2. Preliminary Carbon Impregnated Paper Cylinder Design

A cylinder that did not exhibit large surface irregularities such as possessed by Meyer's cylinder was constructed from a commercially produced resistive paper known as Armstrong Temsheet. Temsheet is a thin, highly flexible, electrically resistive material. It is a carbon impregnated paper containing no wires or ribbons. The nominal thickness is 0.039 inches and the electrical resistance is approximately 25 ohms per square. The heat that is generated when a constant current is passed through the paper is uniform to within two percent from point to point over large areas.

A hollow cylinder with an outer diameter of 3.98 inches and a length of 15 inches was formed from a section of Temsheet.

To hold this cylinder in place two 10 inch long, 4.5 inch outer diameter acrylic tubes were attached to the floor and ceiling of the 32 inch high wind tunnel test section. When placed inside these tubes, the Temsheet cylinder rested on a lip inside the lower cylinder. Two 3.9 inch diameter plugs threaded to a 16 inch center rod were used to force the Temsheet snug against the tubing walls. The longitudinal seam of the Temsheet cylinder was sealed with tape and was placed at 135° from forward stagnation on the side not viewed through the wind tunnel window. The details of construction can be seen in Figure 4.

When assembled, a 12 inch long section of the Temsheet cylinder was located in the center of the wind tunnel

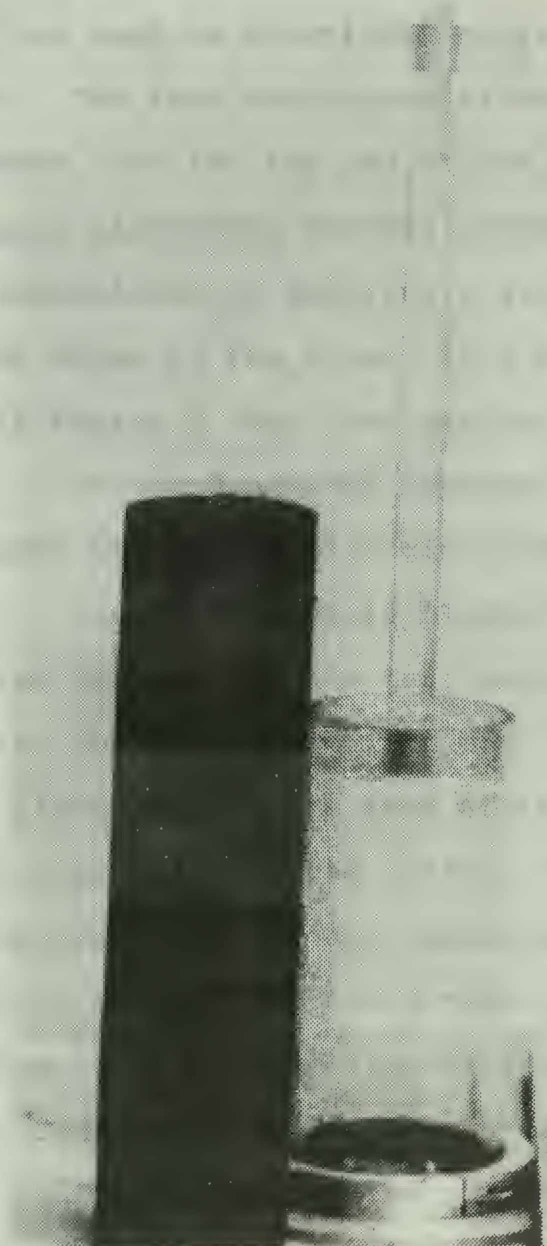

Figure 4. Temsheet Cylinder with Acrylic Tube Holders.

test section. A heat flux was generated by using a Lamba Regulated power supply model LK345A to pass current through the Temsheet.

To insure uniform application of voltage, aluminum tape was used as electrodes on the inner surface of the Temsheet. The tape was placed circumferentially on the surface 2 inches from the top and bottom of the 12 inch test section. Intimate electrical contact between the tape and the Temsheet was established by applying a silver based conducting paint on the edges of the tape. This procedure resulted in a uniformly heated 8 inch test section.

To guard against internal free convection losses the cylinder was filled with glass wool.

Since Temsheet is black, the liquid crystals were applied directly to the test surface. To insure that edge effects would not interfere with readings, no liquid crystals were placed within one inch of the electrodes. See Appendix B for discussion of end losses. The following liquid crystals bands, 3/8 inch wide and separated by 1/8 inch, were painted circumferentially on the surface of the Temsheet cylinder. Reading in order from top to bottom: R-49, S-45, S-43, R-41, S-40, S-38, R-37, S-36, S-34, R-33, S-32, and S-30.

The surface of the cylinder was marked every five degrees to allow one to accurately locate the various isotherms displayed by the liquid crystals.

3. Final Temsheet Cylinder Design

The protruding lips on the acrylic tubes which held the preliminary Temsheet cylinder produced an undesirable secondary flow in the direction of the cylinder axis. This axial velocity component caused the overall flow to be highly three dimensional. Since only two dimensional flow was desired, a new set of supports were designed that exhibited a constant outer diameter to the flow. The final cylinder is shown in Figures 5 and 6.

The upper and lower supports for the Temsheet test section were 3.96 inch diameter wooden cylinders permanently attached to the floor and ceiling of the wind tunnel. The lower cylinder had a one inch diameter hole drilled through its axis to allow the passage of electrical leads.

The wooden cylinders were each 12 inches long with the last 2 inches on the ends turned down approximately .04 inches. This allowed the Temsheet to be attached to the cylinders with double backed tape. The outer diameter of the assembly was then constant over the entire wind tunnel height.

The electrodes were attached as before except that the test section was only 6 inches long.

The following liquid crystals were painted directly on the Temsheet surface; recording from top to bottom: R-49, S-45, S-43, S-40, S-38, S-36, S-34, and S-32.

A second cylinder, utilizing these same bases, was constructed with one crystal, S-43, covering the entire surface from electrode to electrode.

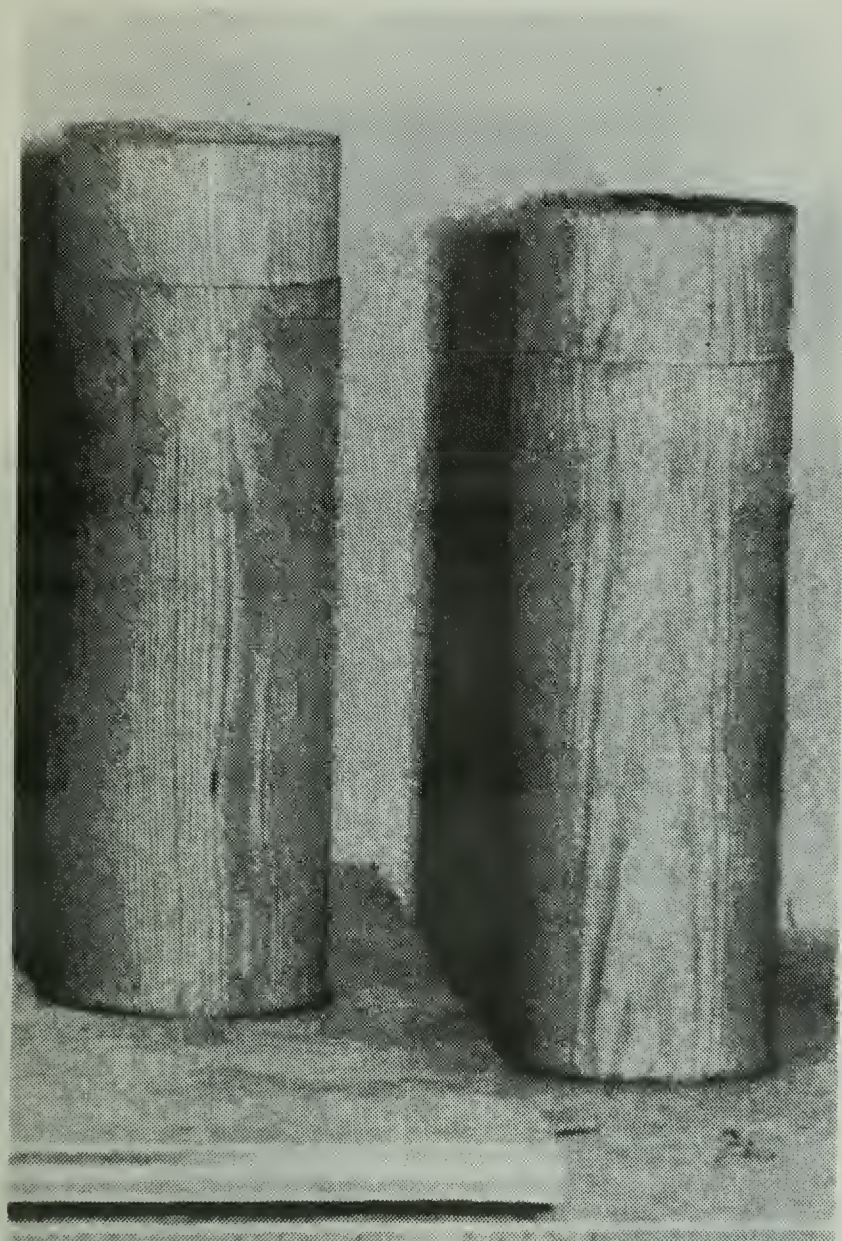

Figure 5. Wooden Bases for Final Temsheet Cylinder.

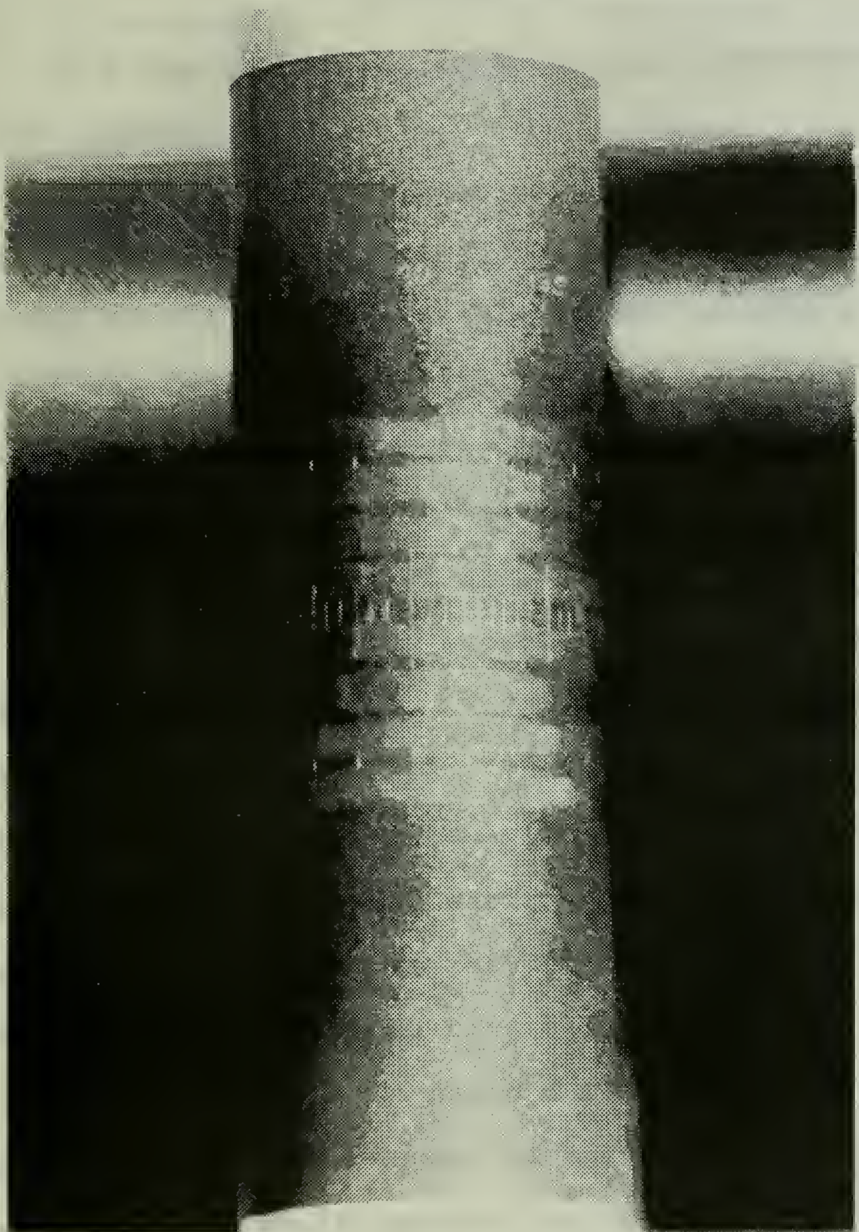

Figure 6. Final Temsheet Cylinder

Finally, both cylinders were marked every five degrees and filled with glass wool as before.

IV. EXPERIMENTAL PROCEDURE

This portion of the investigation consisted of three distinct phases.

Initially, the cylinder used in Meyer's investigation [3] was used to check the liquid crystal readings against those of the installed thermocouples. The procedure outlined by Meyer was used to bring the cylinder to steady state. The liquid crystal temperature display was recorded and thermocouple readings taken at the forward stagnation point and then every 15 degrees of arc.

Some difference was expected between the two temperature distributions obtained. This difference was due to the locations of the two sensors. The thermocouples were located on the inside of the Nichrome ribbon while the liquid crystals read temperature on the surface of the cylinder. Appendix C contains an analysis of the drop in temperature between the thermocouple and liquid crystal surface.

Several items were noted during this phase of experimentation. First, the degree of agreement between thermocouple and liquid crystals depended on noting the point at which a given crystal formulation began its color transition. This was not suprising since calibration procedures mark only the beginning of color transition and a given color may be visible over fractions or multiple degrees Fahrenheit.

Secondly, the surface irregularities caused the creation of local hot and cold spots. This could easily be seen while the cylinder was warming up or when the cylinder was energized with no air flow. Further, the flow pattern in the area of the irregularities was altered. This was visible as small regions of pulsating liquid crystal colors directly behind the irregularity.

Additionally, the number of surface irregularities increased as the number of heating and cooling cycles on the cylinder were increased.

It required approximately 12 hours for Meyer to collect a complete set of thermocouple data. Using the liquid crystals this time could be reduced to approximately two to four hours. Even this was considered too long for practical investigations.

It was decided to construct a new cylinder which would have a smooth surface and allow data to be collected within a reasonable time period.

Before proceeding with a description of the experimental procedure using the Temsheet cylinder, a brief description of the temperature distribution that exists on a uniformly heated cylinder placed in a cross flow of air will be given. This description together with the accompanying Figures 7 and 8 should prove helpful in interpreting the liquid crystal results.

The flow of a real fluid is best analyzed by the changes occurring within the boundary layer that forms near the

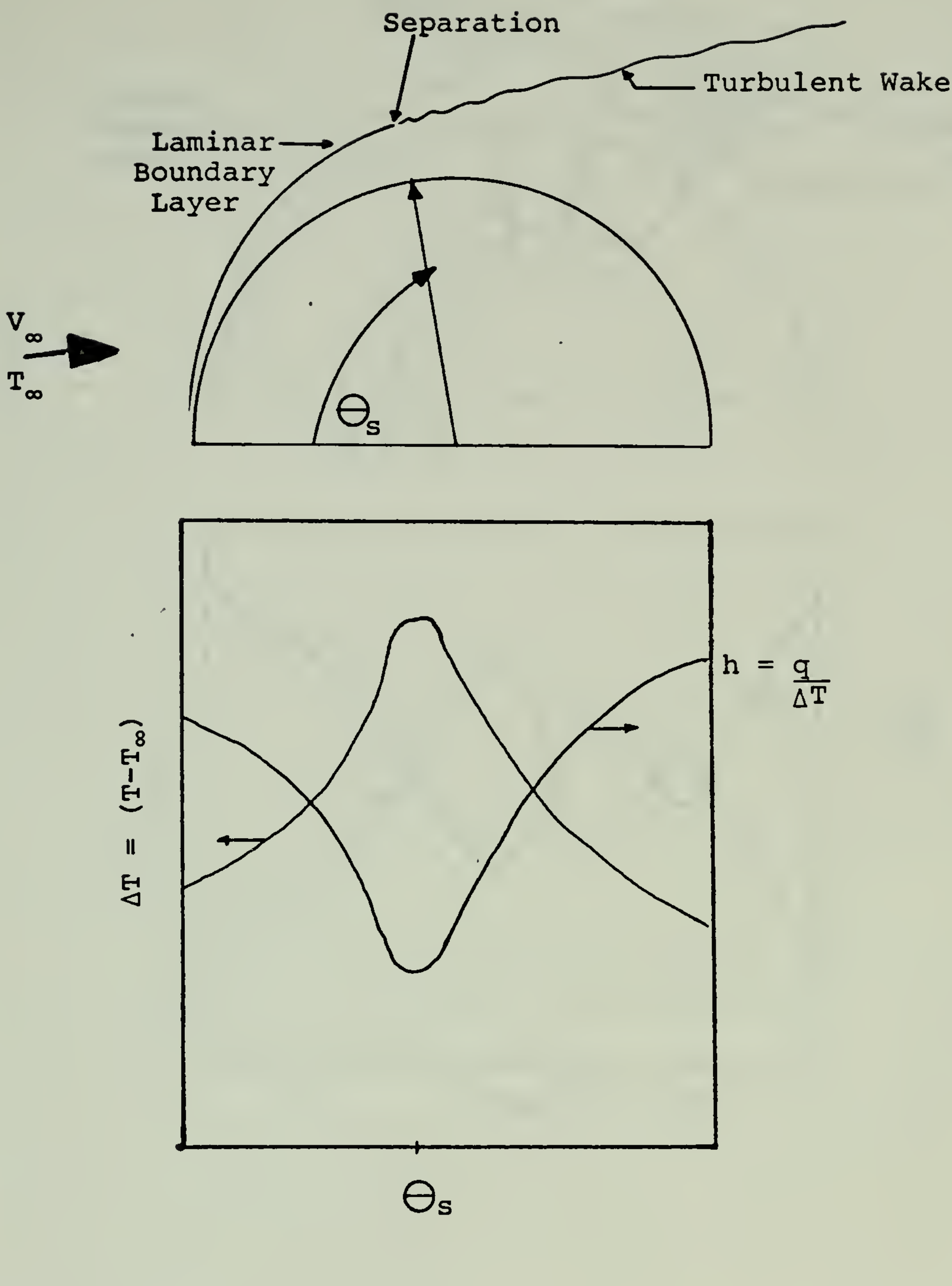

Figure 7. Schematic of a Cylinder in Subcritical Flow with the Resulting Temperature and Heat Transfer Distributions.

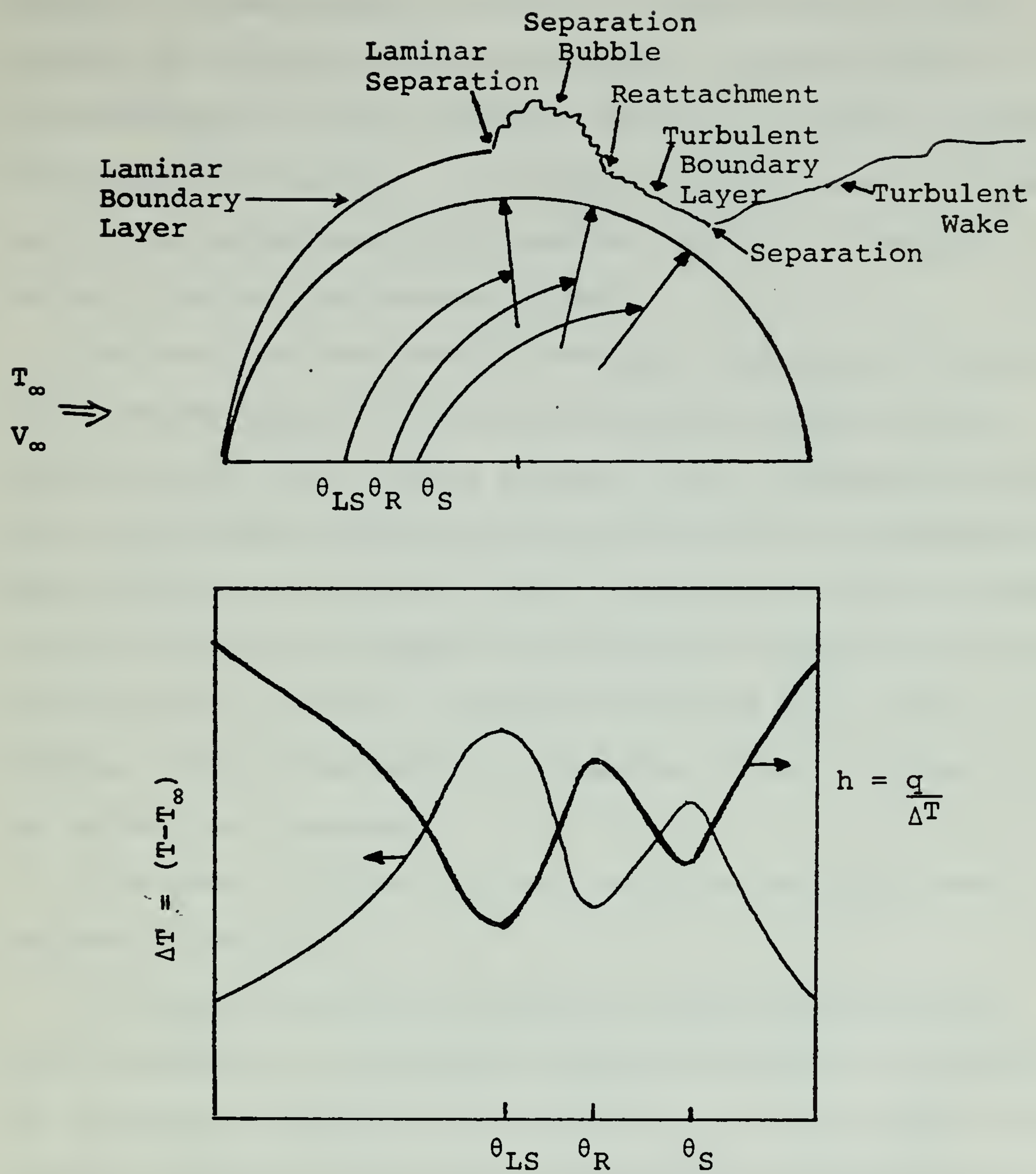

Figure 8. Schematic Diagram of a Cylinder in Critical Flow with the Resulting Temperature and Heat Transfer Distribution

surface. These boundary layers are classified as either laminar or turbulent. The flow within a laminar layer is characterized by fluid particles moving in a smooth, orderly fashion and in layers. A turbulent boundary layer is characterized by individual fluid packets flowing in irregular patterns within the boundary layer.

The heat transfer coefficients and temperature distributions are functions of both the thickness of the boundary layer and the type. As the boundary layer increase in thickness with angular location, the fluid velocity is retarded resulting in an increased thermal resistance to heat transfer. In the case of a uniformly heated cylinder the surface temperature must increase to maintain the wall heat flux at a constant value. The nature of turbulent flow is conductive to better heat transfer.

Flow past a cylinder may be classified as either subcritical or critical.

In subcritical flow the laminar boundary layer grows from a minimum at the forward stagnation point to a maximum at an angular location of 80-85 degrees. At this point the kinetic energy of the fluid is attenuated sufficiently that the adverse pressure gradient present on the surface can no longer be overcome. The laminar boundary layer separates from the surface. The surface is then scrubbed by the turbulent actions of the wake.

Figure 7 depicts a typical subcritical flow pattern and the resulting trends in both temperature and heat transfer

coefficient with angular location. Note that the maximum temperature exists at the separation point. This corresponds to the point of maximum thermal resistance, or minimum heat transfer coefficient.

Critical flow is characterized by an increasing laminar boundary layer thickness on the forward portion of the cylinder just as in the subcritical case. In the vicinity of 80-85 degrees, however, the flow begins a transition from laminar to turbulent flow. The point at which transition begins is known as the laminar separation point. The laminar boundary layer separates but the kinetic energy of the fluid is high enough that the flow reattaches to the surface at some point aft of the laminar separation point. A turbulent boundary layer then develops and finally separates from the surface in the region of 110-130 degrees (the actual point of reattachment and ultimate separation is a function of the Reynolds number).

Figure 8 depicts the critical flow pattern and the resulting trends in both temperature and heat transfer coefficient with angular location.

The development of a consistent method of obtaining accurate heat transfer data with liquid crystals was the objective of the next phase of experimentation. The temperature fields that existed on the Temsheet cylinder held by acrylic tubes were observed under steady state conditions in the wind tunnel. The best procedure for obtaining accurate information was developed by analyzing the visual temperature

fields and comparing them with those of the previously discussed theory of angular temperature and heat transfer distributions.

As noted earlier, the most accurate temperatures were found at the beginning of color transitions on the liquid crystals. In areas of large temperature gradients there was no problem in determining the start of red, green, or blue. The particular liquid crystal in the temperature range at these points would undergo the red to green to blue transition in a short interval. The point of blue transition was easily noted.

The point of transition in the area of stagnation was much more difficult to observe. The temperature gradients in this region were very shallow. It was not uncommon for one liquid crystal to exhibit approximately the same color over 15 to 20 degrees of arc. The actual transition to this color was usually not apparent. The error in reading a temperature in this region could be as large as 1°F. To obtain a precise temperature the beginning of a transition was forced by adjusting the power supply until a previously unchanged liquid crystal just began its transition. This was verified by decreasing the voltage a few tenths of a volt and observing the liquid crystal return to its previous color.

If a clear cut transition from red to green, or green to blue occurred in any region of shallow temperature gradients, it was considered precise and used. This type of transition

usually occurred in angular regions 15 to 60 degrees aft of the forward stagnation point.

The hottest point on the cylinder surface was at separation (Figure 7). This point was found by adjusting voltage until the first point of red color was observed on an unchanged crystal or decreasing power on one that was already through its transition until the very last red point remained. The location was checked by repeating the procedure on a different liquid crystal band. The two points invariably fell on a vertical line.

By combining the procedures repeatable results were obtained for a given Reynolds number.

While experimenting with the above procedure the Reynolds number was maintained at approximately 50,000, clearly in the subcritical flow regime. However, a local cold spot not attributable to normal subcritical flow patterns existed in the region of 90 degrees. Small strings placed on the cylinder confirmed that undesirable secondary flow patterns were generated by the lips on the acrylic tubes. Due to this flow anomaly a third phase of experimentation employing an improved wooden base was initiated. The objective of the third phase of the investigation was to gather data for comparison with conventional works. This was done in three steps. The new wooden base Temsheet cylinder was tested for two dimensional flow characteristics and edge losses. The roughness of the Temsheet and liquid crystal coatings were examined. Data for Reynolds numbers ranging from 38,000 to 148,000 were obtained for analysis.

For data collection the Temsheet cylinder with eight liquid crystal bands was installed in the wind tunnel.

The airstream thermocouple and its reference ice bath were inspected and temperature recorded for initial calculation of airstream properties and velocity.

A U-tube manometer and micromanometer used for airspeed indication were carefully zeroed.

The power supply was energized and voltage adjusted to cause all liquid crystal bands to undergo a transition. This served two purposes. First, if the glass wool packing was not installed snuggly a point of temperature discontinuity would appear. The packing could then be adjusted prior to establishing air flow. Secondly, the cylinder could be preheated to reduce the time necessary to reach steady state.

The wind tunnel was started and the air speed was increased using the previously calculated pressure drop on the U-tube manometer.

Since the U-tube manometer was not very sensitive over the entire range of Reynolds numbers, especially at the lower Reynolds numbers, the pressure drop read on the micromanometer was used to recalculate air speed and Reynolds number. This proved to be a critical part of the experiment.

Power was increased until the upper liquid crystal, R-49, began its red transition at separation. Power was continually adjusted to maintain red at separation until steady state was reached. This usually occurred within fifteen minutes and was typified by a period of approximately five

or more minutes of a constant red without adjusting power. This was checked by decreasing power a few tenths of a volt and noting the red spot disappear.

Data were collected after restoring power to its previous setting. The angular location of each liquid crystal color transition, voltage, airstream temperature, and micromanometer height were recorded.

For critical flows the procedure for locating separation was followed to locate the points of laminar separation, reattachment, and final separation.

The test for edge effects and two dimensional flow characteristics consisted of placing a Temsheet cylinder coated with liquid crystal S-43 from electrode to electrode in the wind tunnel.

The wind tunnel was started and the cylinder heated to steady state. The isotherms were then observed for straightness and end effects.

Although the surface of the Temsheet was smooth to the touch the actual surface roughness and effects of the liquid crystals were not known. A piece of Temsheet coated with liquid crystals was examined under an electron microscope.

V. RESULTS

A. TEMPERATURE DISTRIBUTION AND HEAT TRANSFER

The numerical data and data reduction technique are contained in Appendix A. Briefly, the local heat transfer coefficient was obtained by dividing the heat generated per unit area by the temperature difference between the surface and airstream temperatures.

$$h = q/\Delta T$$

The value of q was determined by dividing electrical power generated by the surface area

$$q = \frac{(V^2/R)}{A}$$

The local convective heat transfer coefficient, h_c, was then obtained by subtracting the radiation coefficient, h_r, (see Appendix A) from h.

$$h_c = h - h_r$$

The Nusselt number (Nu) was calculated using the expression

$$Nu = \frac{h_c D}{k}$$

and the Froessling number calculated from

$$Fr = \frac{Nu}{\sqrt{Re}}$$

Data are presented graphically in this section. Figures of temperature distribution, Nusselt numbers, and Froessling numbers are included.

Figure 9 shows a sketch of a typical subcritical flow temperature distribution and a representation of the isotherms seen on the liquid crystal bands on the cylinder surface.

Critical flow was noted at a Reynolds number of approximately 120,000. The shape of a typical critical flow temperature distribution was shown in Figure 8. Figure 10 is a color photo of the actual temperature distribution on the cylinder surface for this critical flow condition. Note that on the upper liquid crystal band, R-49, the presence of the separation region is characterized by a maximum temperature at 115° (denoted by a red patch) with lower temperatures on either side (denoted by black). The blue region forward of this region indicate higher temperatures and bracket the laminar separation point.

The Nusselt numbers for several Reynolds numbers are plotted in Figure 11. Several items should be noted from these curves.

First, the general shape of the curves is consistent with the previous work of Giedt and Meyer [2,3] in both critical and subcritical flows.

The points of minimum heat transfer coefficients occur in the region of 80 to 90°. However, unlike the work of Giedt, these points move forward on the cylinder with increasing Reynolds numbers. This may be due to a slight deformation of the cylinder as velocity increases. Deformation was not visible to the naked eye at Reynolds numbers below 150,000. It was interesting to note that the isotherms

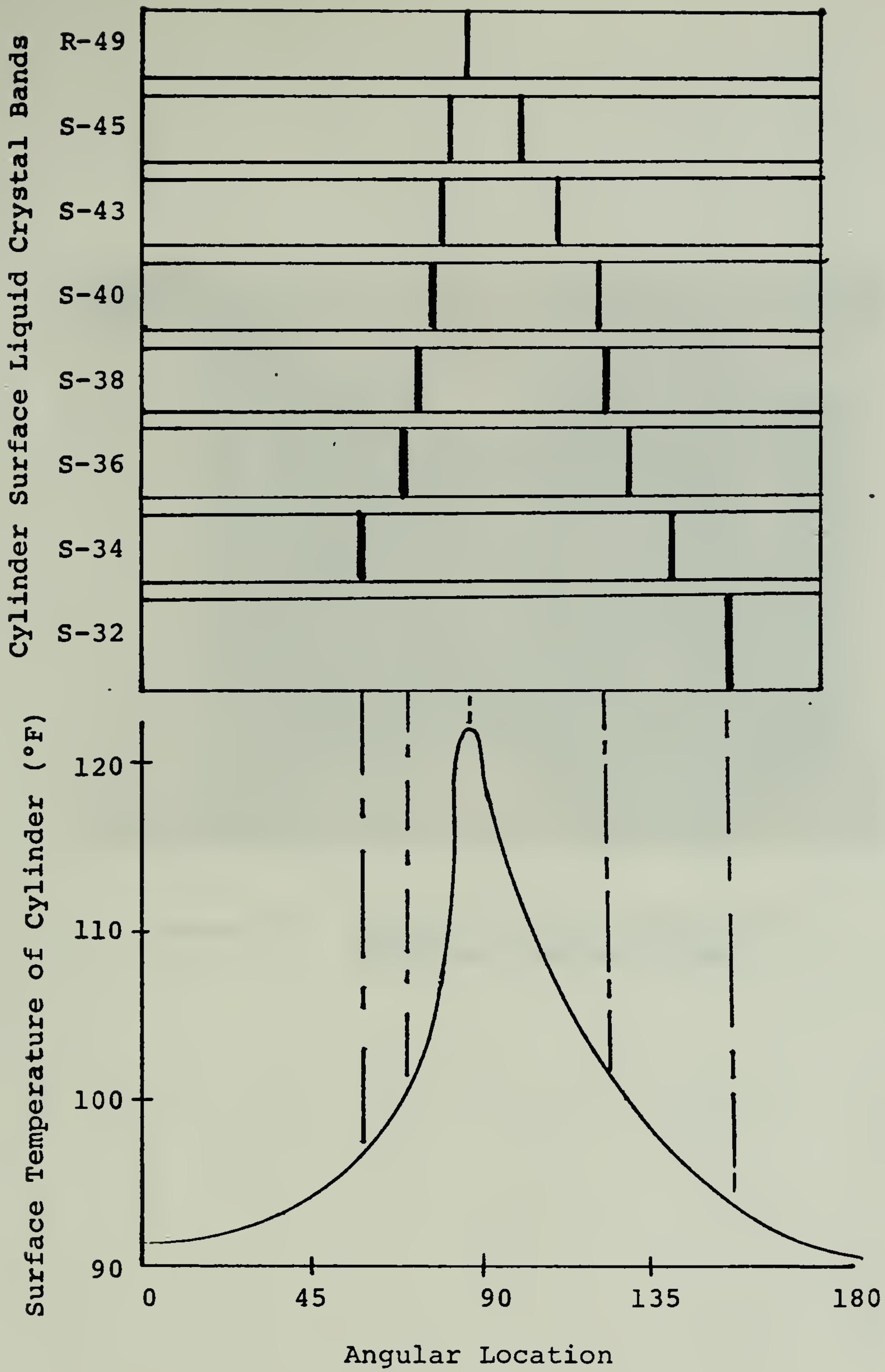

Figure 9. Liquid Crystal Temperature Field and Resulting Temperature Distribution on the Cylinder Surface. Subcritical flow conditions indicated.

Figure 10. Liquid Crystal Temperature Field in Critical Flow.

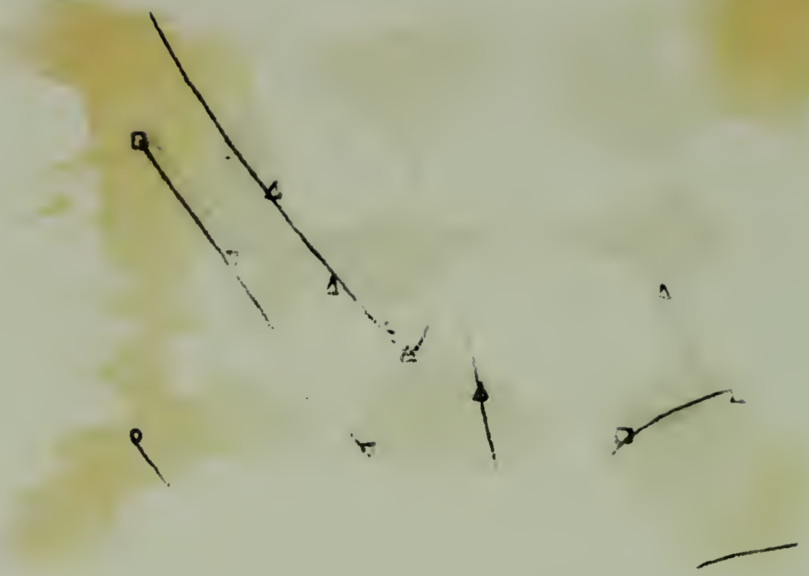

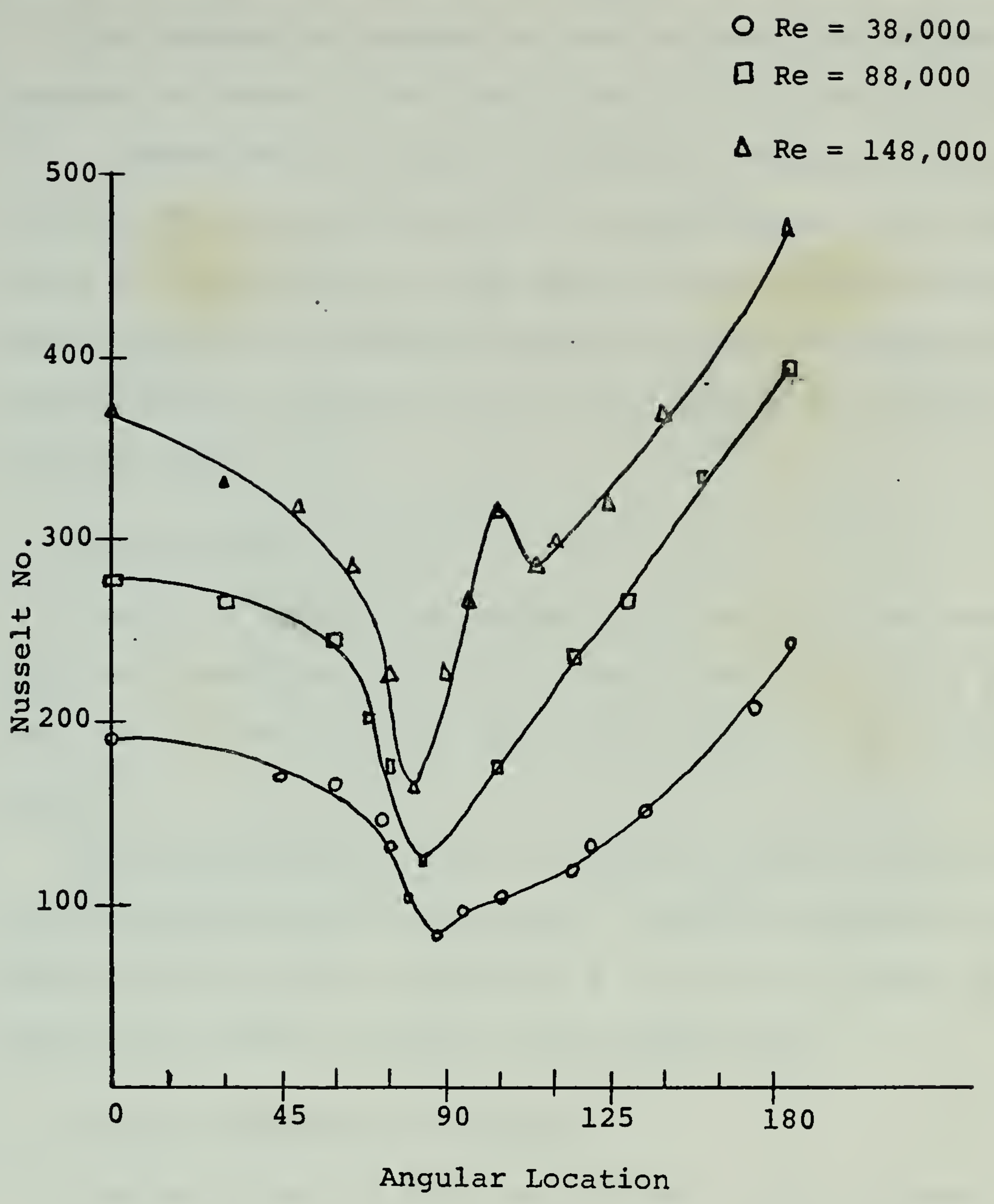

Figure 11. Heat Transfer Results at Reynolds Numbers of 38,000, 88,000, and 148,000.

depicted on the cylinder surface were no longer vertical when deformation was visible. This can be seen in Figure 12.

The Froessling numbers for the laminar flow regions are plotted in Figure 13 for comparison with the theory of Schuh [1]. Comparison is within experimental uncertainty near stagnation and then drops off near separation. The latter trend is consistent with the work of Giedt and is most probably explained by the fact that Schuh used an ideal pressure distribution as opposed to the distribution encountered in viscous flows.

B. EDGE EFFECTS

Figure 14 showed the isotherms on the cylinder coated with one liquid crystal, S-43. They clearly indicate that heat is lost near the top and bottom edges of the coated region.

The edge effects are indicated by a slight curvature of the isotherms near the electrodes. This is expected from the model developed in Appendix B and was the reason for not taking data within an inch of the electrodes.

C. SURFACE ROUGHNESS OF TEMSHEET

Figures 15 and 16 show the Temsheet liquid crystal interface magnified 121 and 27 times respectively. The point to note is that the liquid crystals fill-in irregularities in the surface and appear to be 20-30 micron spheres as specified by the manufacturer.

Figure 12. Cylinder Deformation at Reynolds Numbers Greater than 150,000.

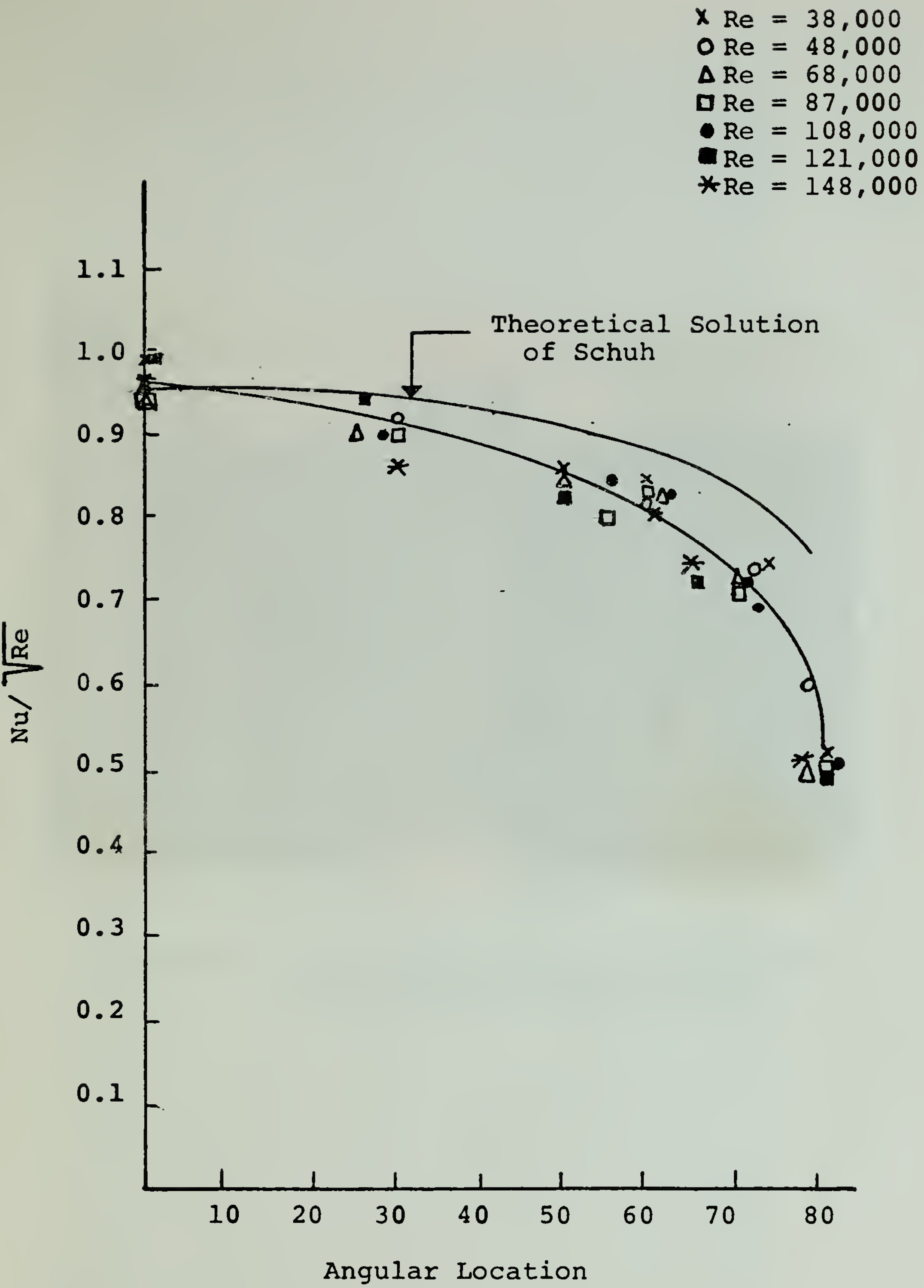

Figure 13. Comparison of Experimental Results of the Present Investigation with the Theoretical Solution of Schuh.

Figure 14. Isotherms Showing End Losses and Two Dimensional Flow Pattern.

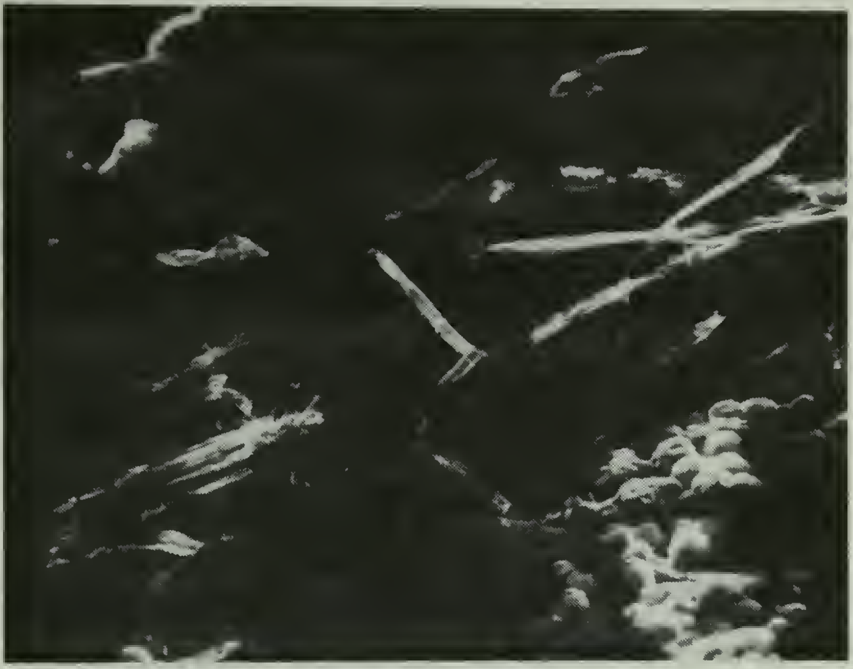

Figure 15. Temsheet-Liquid Crystal Surface at 121X.

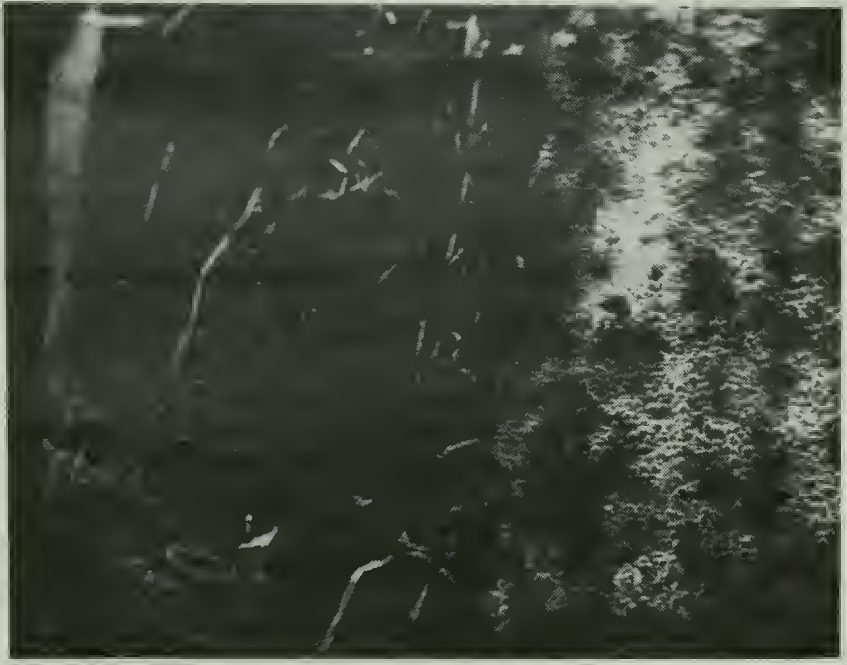

Figure 16. Temsheet-Liquid Crystal Surface at 27X.

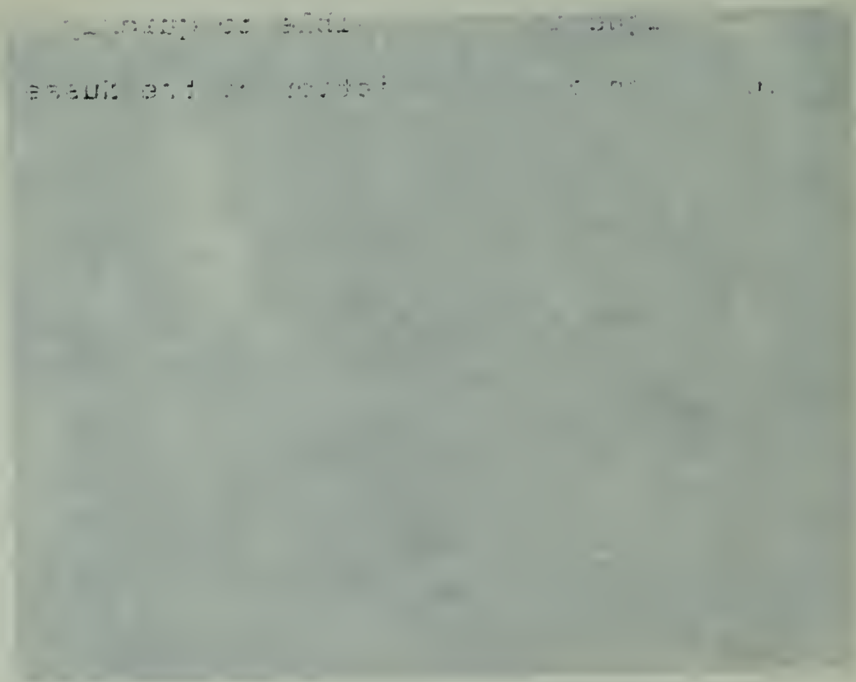

Fage and Warsap in reference 18 predict a transition to critical flow at a Reynolds number of approximately 148,000 for flow over a cylinder with a surface roughness equivalent to the roughness of the crystal coated Temsheet ($k/D=2\times10^{-4}$); k being the critical roughness height and D the diameter of the cylinder. The actual transition occurred at approximately 120,000.

VI. CONCLUSIONS AND RECOMMENDATIONS

The liquid crystal thermographic technique developed in this investigation provides an excellent means of obtaining both qualitative and quantitative heat transfer information on heated objects placed in forced convection environments. Using the technique it was possible to quickly and easily obtain information on the variation of the Nusselt number around the circumference of a uniformly heated right circular cylinder placed in a cross flow of air. The technique also allowed one to visually observe the effects of flow separation, the turbulent boundary layer, and the turbulent wake on the surface temperature of the cylinder. Colored movies taken of a cylinder coated with a single liquid crystal are especially vivid in their display of the influence of the turbulent wake on the cylinder surface temperature. In the wake region the crystals alternately dim and glow in response to the "scrubbing" action caused by random bursts of cool fluid impacting on the surface.

The ability to visually observe turbulent flow pattern effects on surface temperatures suggests an excellent means for studying the influence of free stream turbulence on the heat transfer rates of heated objects. However, in order that such a study be conducted in a quantitative manner, the thermal response time of the liquid crystals must first be determined. Parker [19], using a capacitor discharge technique, found that a 0.001 inch film of liquid crystals coated on a thin stainless steel foil responded in approximately 0.036 seconds to a step change in foil temperature. It is possible that a thin coat of liquid crystals placed on a material such as Temsheet would respond even faster than this due to the fact that the crystals are partially absorbed by the Temsheet. The ideal situation would be if the liquid crystals responded at the same rate as the Temsheet itself. An experiment, similar to the one conducted by Parker, needs to be conducted to determine response time information on the liquid crystals.

As a final recommendation, the phenomenon shown in Figure 17 is offered as a possible topic for future investigation. During the final phase of collecting wind tunnel data for the present investigation, it was noted that the cylinder coated with liquid crystal S-43 displayed alternate hot and cold spots along the separation line. These spots were uniformly spaced and seemed to be caused by some flow phenomenon, perhaps a series of vortices such as one observes in flow in a curved channel. Whatever the cause, the hot and cold spots

Figure 17. Hot and Cold Spots on the Cylinder Surface along Separation Line.

definitely existed as is readily apparent in Figure 17. Precise measurements were not taken at the time the phenomenon was observed (the Reynolds number was approximately 75,000) and no explanation is offered for its existence. It should be noted, however, that such a phenomenon may well have gone undetected if thermocouples were used as the temperature sensor. Additional research, perhaps using liquid crystals for temperature sensing and smoke for flow visualization, needs to be conducted to explain the observed phenomenon.

APPENDIX A

DATA AND DATA REDUCTION

In order to experimentally determine the Nusselt number as a function of angular location on the right circular cylinder under investigation, a relationship between the convective heat transfer coefficient, h_c, and the surface heat flux produced by the Joulean heating effect in the Temsheet, V^2/RA, was needed. This relationship is easily developed by performing a simple energy balance on an elemental volume, see Giedt [2] or Meyer [3]. The result is

$$h_c = \frac{\frac{V^2}{RA} + \frac{kt}{r_o^2}\frac{dT^2}{d\theta^2}}{(T-T_\infty)} - h_r$$

where

h_c = Convective heat transfer coefficient

V = Voltage impressed across the test section

R = Electrical resistance of test section

A = Area of test section

t = Thickness of test section

k = Thermal conductivity of test section material

r_o = Radius of the cylinder

T = Temperature at angular location θ

θ = Angular location

T_∞ = Air stream temperature

h_r = Radiation heat transfer coefficient = $\sigma F_{1-2}\{T+T_\infty\}\{T^2+T_\infty^2\}$

F_{1-2} = Radiation exchange factor between cylinder and surroundings

σ = Stefan-Boltzman Constant

An exact value for thermal conductivity of the Temsheet material was not available, but assuming that its value is approximately the same as other carbon paper products, the product kt is calculated to be .000195 BTU/hr-°F. Since this value is so low it was felt that the conduction term in the expression for convective coefficient could be neglected. The expression used for the convective coefficient then takes the final form:

$$h_c = \frac{V^2}{RA(T-T_\infty)} - h_r$$

The Nusselt number is:

$$Nu = \frac{2h_c r_o}{k_{air}}$$

The Froessling number is:

$$Fr = Nu/\sqrt{Re}$$

where

Re = Reynolds number = $V_\infty D/\nu$

V_∞ = Air velocity

ν = Air kinematic viscosity

A sample calculation is provided for illustration using the following values from the data at a Reynolds number 47,818:

θ = 60°

ε = .9

σ = $.1714 \times 10^{-8}$ BTU/hr-ft^2-°R^4

T_∞ = 62.7°F

T = 96.3°F

V_∞ = 22.5 ft/sec

V = 23.7 Volts

R = 12.0 Ω

$$D/K = 22\ \frac{\text{hr-°F-ft}^2}{\text{BTU}}$$

Re = 47,818

$$h = \frac{(23.7V)^2}{(12.0\Omega)(.52\text{ft}^2)(33.6°\text{F})(.293\text{WATTS/BTU/hr}}$$

$$h = 9.2\ \frac{\text{BTU}}{\text{hr-ft}^2\text{-°F}}$$

$$h_r = .9(.1714 \times 10^{-8}\text{BTU/hr-ft}^2\text{-°R}^4)(556.3+522.7)(556.3^2+552.7^2)\,°\text{R}^3$$

$$h_r = .97\ \frac{\text{BTU}}{\text{hr-ft}^2\text{-°F}}$$

$$h = 8.2\ \frac{\text{BTU}}{\text{hr-ft}^2\text{-°F}}$$

$$Nu = \left(8.2\ \frac{\text{BTU}}{\text{hr-ft}^2\text{-°F}}\right)\left(22\ \frac{\text{hr-°F-ft}^2}{\text{BTU}}\right)$$

Nu = 180.4

$$Fr = \frac{180.4}{\sqrt{47,818}} = .82$$

The data sheets for all seven Reynolds numbers investigated follow.

DATA

Air Temp. = 65.5°F; D/ν = 2050 $\frac{\text{sec}}{\text{ft}}$

Air Speed = .19 cmH_2O

= 18 ft/sec

Re = 36900

Correction Factor = 1.0267

Re_{corr} = 37,885

Voltage = 25.6 V

Heat Flux = 359 BTU/hr.ft²

Film Temp = 90 °F; D/K = 21.8 $\frac{\text{hr-°F-ft}^2}{\text{BTU}}$

Date: 1-25-74

Time: 1645

Crystal reader: FIELD

Data sheet: Cooper

Cylinder Dia. = .33 ft

Cylinder Area = .519

Resistance = 12 Ω

Crystals:

R49	538
545	536
543	534
540	532

θ	CRY.	TEMP (°F)	ΔT	h	h_r	h_c	Nu	F_R	Comments
0	538G	102.4	36.9	9.73	1.00	8.73	190	.98	
60	540B	107.1	41.6	8.62	1.01	7.61	166	.85	
73	543B	112.3	46.8	7.67	1.03	6.64	145	.75	
74	545B	115.1	49.6	7.23	1.04	6.19	135	.69	
77	R49B	121.7	56.2	6.39	1.05	5.34	116	.6	
103	R49B	121.7	56.2	6.39	1.05	5.34	116	.6	
130	545B	115.1	49.6	7.23	1.04	6.19	135		
137	543B	112.3	46.8	7.67	1.03	6.64	145		
145	540B	107.1	41.6	8.62	1.01	7.61	166		
155	538B	103.9	38.4	9.35	1.00	8.35	182		
165	536B	99.4	33.9	10.59	.99	9.60	209		
180	534G	95.2	29.7	120.9	.98	11.11	242		
CHANGED VOLTAGE., V = 22.1, q = 267, T∞ = 65.5, R = 12.0									
50	534B	96.3	30.8	8.67	.98	7.69	168	.86	
65	536B	99.9	33.9	7.88	.99	6.89	150	.77	
75	538B	103.9	38.4	6.95	1.00	5.95	129.7	.67	
78	540B	107.1	41.6	6.42	1.01	5.41	118	.61	
82	543B	112.3	46.8	5.71	1.03	4.68	102	.52	
84	545B	115.1	49.6	5.38	1.04	4.34	95	.49	
87	R49B	121.7	56.2	4.75	1.05	3.7	81	.42	← SEPARATION
100	545B	115.1	49.6	5.38	1.04	4.34	95		
105	543B	112.3	46.8	5.71	1.03	4.68	102		
124	540B	107.1	41.6	6.42	1.01	5.41	118		
130	538B	103.9	38.4	6.95	1.00	5.95	130		
145	536B	99.4	33.9	7.88	.99	6.89	150		
155	534B	96.3	30.8	8.67	.98	7.69	168		
165	532B	92.6	27.1	9.85	.97	8.88	194		

D A T A

Air Temp. = 62.7 °F; D/ν = 2070 $\frac{sec}{ft}$

Air Speed = 0.29 cmH_2O

= 22.5 ft/sec

Re = 46,575

Correction Factor = 1.0267

Re_{corr} = 47,818

Voltage = 23.7 V

Heat Flux = 308 $BTU/hr.ft^2$

Film Temp = 85 °F; D/K = 22 $\frac{hr\text{-}°F\text{-}ft^2}{BTU}$

Date: 1-26-74

Time: 1000

Crystal reader: FIELD

Data sheet: COOPER

Cylinder Dia. = 0.330 FT

Cylinder Area = 0.519 FT^2

Resistance = 12.0 Ω

Crystals:

R49 S38

S45 S36

S43 S34

S40 S32

θ	CRY.	TEMP (°F)	ΔT	h	h_r	h_c	Nu	F_R	Comments
60	S-34B	96.3	33.6	9.17	.97	8.2	180.4	.82	
72	S-36B	99.4	36.7	8.39	.98	7.41	163	.74	
76	S38B	103.9	41.2	7.48	.99	6.49	143	.65	
79	S40B	107.1	44.4	6.94	1.00	5.94	131	.6	
82	S43B	112.3	49.6	6.21	1.01	5.2	114	.52	
84	S45B	115.1	524	5.88	1.02	4.86	107	.49	
87	R49R	121.7	59.0	5.22	1.04	4.18	92		← SEPARATION
97	S45B	115.1	52.4	5.88	1.02	4.86	107		SUBCRITICAL FLOW
102	S43B	112.3	49.6	6.21	1.01	5.2	114		NO BUBBLE
113	S40B	107.1	44.4	6.94	1.00	5.94	131		
122	S38B	103.9	41.2	7.48	.99	6.49	143		
132	S36B	99.4	36.7	8.39	.98	7.41	163		
140	S34B	96.3	33.6	9.17	.97	8.2	180.4		
155	S32B	92.6	29.9	10.30	.96	9.34	205		
	CHANGED VOLTAGE TO 27.6 V, q = 417						T_∞ = 62.7		
0	S38G	102.4	39.7	10.50	.99	9.51	209	.95	
62	S40B	107.1	44.4	9.39	1.00	8.39	185	.84	
72	S43B	112.3	49.6	8.41	1.01	7.4	163	.74	
74	S45B	115.1	52.4	7.96	1.02	6.94	153	.7	
77	R49B	124.2	61.5	6.78	1.05	5.73	126	.58	
104	R49B	124.2	61.5	6.78	1.05	5.73	126		
130	S45B	115.1	52.4	7.96	1.02	6.94	153		
134	S43B	112.3	49.6	8.41	1.01	7.40	163		
142	S40B	107.1	44.4	9.39	1.00	8.39	185		
150	S38B	103.9	41.2	10.12	.99	9.13	201		
157	S36B	99.4	36.7	11.36	.98	10.38	228		
180	S34G	95.2	32.5	12.83	.96	11.87	261		
30°	S38B	103.9	41.2	10.12	.99	9.13	201	.92	

DATA

Air Temp. = 63.4 °F; D/ν = 2070 $\frac{sec}{ft}$

Air Speed = .6 cmH_2O

= 32 ft/sec

Re = 66,240

Correction Factor = 1.0267

Re_{corr} = 68,008

Voltage = 29.5 V

Heat Flux = 477 BTU/hr.ft²

Film Temp = 88 °F; D/K = 21.8 $\frac{hr\text{-}°F\text{-}ft^2}{BTU}$

Date: 1-26-74

Time: 1115

Crystal reader: FIELD

Data sheet: COOPER

Cylinder Dia. = .33 ft

Cylinder Area = .519 ft²

Resistance = 12.0 Ω

Crystals:

R49 S38
S45 S36
S43 S34
S40 S32

θ	CRY.	TEMP (°F)	ΔT	h	h_r	h_c	Nu	F_R	Comments
0	S38G	102.4	39.0	12.23	.99	11.24	245	.94	
25	S38B	103.9	40.5	11.78	.99	10.79	235	.9	
51	S40G	106.1	42.7	11.17	1.00	10.17	222	.85	
59	S40B	107.1	43.7	10.92	1.00	9.92	216	.83	
70	S43B	112.3	48.9	9.75	1.02	8.73	190	.73	
73	S45B	115.1	51.7	9.23	1.04	8.19	179	.69	
77	R49B	124.2	60.8	7.85	1.05	6.8	148	.57	
103	R49B	124.2	60.8	7.85	1.05	6.8	148		
120	S45B	115.1	51.7	9.23	1.04	8.19	179		
126	S43B	112.3	48.9	9.75	1.02	8.73	190		
135	S40B	107.1	43.7	10.92	1.00	9.92	216		
145	S38B	103.9	40.5	11.78	.99	10.79	235		
155	S36B	99.4	36.0	13.25	.98	12.27	267		
165	S34B	96.3	32.9	14.5	.97	13.5	301		
180	S32G	92.6	29.2	16.34	.96	15.38	335		<- CHANGED
55	S34B	96.3	32.9	10.67	.97	9.7	211	.81	VOLTAGE
67	S36B	99.4	36	9.75	.98	8.77	191	.73	V=25.3V
70	S38B	103.9	40.5	8.67	.99	7.68	167	.64	T_∞=63.4°F
74	S40B	107.1	43.7	8.03	1.00	7.03	153	.59	q = 351
76	S43B	112.3	48.9	7.18	1.02	6.16	134	.51	
78	S45B	115.1	51.7	6.79	1.04	5.75	125	.5	
85	R49B	121.7	58.3	6.02	1.05	4.97	108		<- SEPARATION
100	S45B	115.1	51.7	6.79	1.04	5.75	125		
102	S43B	112.3	48.9	7.18	1.02	6.16	134		
108	S40B	107.1	43.7	8.03	1.00	7.03	153		
124	S36B	99.4	36.0	9.75	.98	8.77	191		
130	S34B	96.3	32.9	10.67	.97	9.7	211		
143	S32B	92.6	29.2	12.02	.96	11.06	241		

DATA

Air Temp. = 64.1 °F; $^{D}/_{\nu}$ = 2060 $\frac{sec}{ft}$

Air Speed = 1.5 cmH_2O

= 51 ft/sec

Re = 105,060

Correction Factor = 1.0267

Re_{corr} = 107,865

Voltage = 32.5 V

Heat Flux = 579 BTU/hr.ft^2

Film Temp = 88 °F; $^{D}/_{K}$ = 21.8 $\frac{hr\text{-}°F\text{-}ft^2}{BTU}$

Date: 1-26-74

Time: 1325

Crystal reader: FIELD

Data sheet: COOPER

Cylinder Dia. = .33 ft

Cylinder Area = .519 ft^2

Resistance = 12.0

Crystals:

R49	538
545	536
543	534
540	532

θ	CRY.	TEMP (°F)	ΔT	h	h_r	h_c	Nu	F_R	Comments
0	538G	102.4	38.3	15.12	.99	14.13	308	.94	
28	538B	103.9	39.8	14.55	.99	13.56	296	.90	
56	540G	106.1	42.0	13.79	1.00	12.79	279	.85	
60	540B	107.1	43	13.47	1.00	12.47	272	.83	
70	543B	112.3	48.2	12.01	1.01	11.00	240	.73	
73	545B	115.1	51.0	11.35	1.02	10.33	225	.69	
77	R49B	124.2	60.1	9.6	1.05	8.55	186	.57	
102	R49B	124.2	60.1	9.6	1.05	8.55	186		
105	545B	115.1	51.0	11.35	1.02	10.33	225		
112	543B	112.3	48.2	12.01	1.01	11.00	240		
122	540B	107.1	43	13.47	1.00	12.47	272		
125	538B	103.9	39.8	14.55	.99	13.56	296		
145	536B	99.4	35.3	16.4	.98	15.42	336		
155	534B	96.3	32.2	17.98	.97	17.01	371		
180	532R	90.5	26.4	21.93	.96	20.97	457		← CHANGED
55	534B	96.3	32.2	13.26	.97	12.29	268	.82	VOLTAGE
65	536B	99.4	35.3	12.1	.98	11.12	242	.74	V=27.9
75	538B	103.9	39.8	10.73	.99	9.74	212	.65	T_∞=64.1
77	540B	107.1	43	9.93	1.00	8.93	183	.56	q=427
80	543B	112.3	48.2	8.87	1.01	7.85	171	.52	R=12.0
81	545B	115.1	51.0	8.37	1.02	7.35	160	.49	
83	R49R	121.7	57.6	7.4	1.04	6.36	139		← SEPARATION
95	545B	115.1	51.0	8.37	1.02	7.35	160		NO BUBBLE
96	543B	112.3	48.2	8.86	1.01	7.85	171		SUBCRITICAL
101	540B	107.1	43	9.93	1.00	8.93	182		
107	538B	103.9	39.8	10.73	.99	9.74	212		
112	536B	99.4	35.3	12.1	.98	11.12	242		
120	534B	96.3	32.2	13.26	.97	12.29	268		

D A T A

Air Temp. = 67.1 °F; $D/_{\nu}$ = 2040 $\frac{\text{sec}}{\text{ft}}$

Air Speed = 1.92 cmH_2O

= 58 ft/sec

Re = 118,320

Correction Factor = 1.0267

Re_{corr} = 121,479

Voltage = V

Heat Flux = $BTU/hr.ft^2$

Film Temp = 88.5°F; $D/_{K}$ = 22 $\frac{hr\text{-}°F\text{-}ft^2}{BTU}$

Date: 1-26-74

Time: 1515

Crystal reader: FIELD

Data sheet: COOPER

Cylinder Dia. = .33 ft

Cylinder Area = .519 ft^2

Resistance = 12.0

Crystals:

R49 S38
S45 S36
S43 S34
S40 S32

θ	CRY.	TEMP (°F)	ΔT	h	h_r	h_c	Nu	F_R	Comments
		VOLTAGE	= 37.2	T∞ = 67.1		q =	758		START OF
~109	R49G	122	54.9	13.81	1.05	12.76	281		CRITICAL FLOW
112	R49B	124.2	57.1	13.27	1.05	12.22	269		← MIN TEMP
107	R49B	124.2	57.1	13.27	1.05	12.22	269		← MAX TEMP
67	R49B	124.2	57.1	13.27	1.05	12.22	269	.77	2nd SEPERATION
130	S45B	115.1	48	15.79	1.04	14.75	325		
142	S43B	112.3	45.2	16.77	1.03	15.74	346		
150	S40B	107.1	40	18.95	1.01	17.94	395		
180	S38R	101.4	34.3	22.1	1.00	21.1	464		
	VOLTAGE	= 27.3V		T∞ =	67.1°F	, q	= 408		
55	S34B	96.3	29.2	13.97	.98	12.99	286	.82	
66	S36B	99.4	32.3	12.63	.99	11.64	256	.74	
74	S38B	103.9	36.8	11.09	1.00	10.09	222	.64	
76	S40B	107.1	40	10.2	1.01	9.19	202	.58	
78	S43B	112.3	45.2	9.03	1.03	8.00	176	.51	
82	R49R	121.7	54.6	7.47	1.05	6.42	141		← 1ST
95	S43B	112.3	45.2	9.03	1.03	8.00	176		SEPARATION
98	S40B	107.1	40	10.2	1.01	9.19	202		
104	S38B	103.9	36.8	11.09	1.00	10.09	222		
112	S36B	99.4	32.3	12.63	.99	11.64	256		
120	S34B	96.3	29.2	13.97	.98	12.99	286		
135	S32B	92.6	25.5	16.00	.97	15.03	331		
		VOLTAGE	= 30.6	, T∞ = 67.1°F			q = 513		
0	S36G	98.2	31.2	16.44	.99	15.45	340	.98	
26	S36B	99.4	32.3	15.88	.99	14.89	328	.94	
50	S38B	103.9	36.8	13.94	1.00	12.94	285	.82	
160	S32B	92.6	25.5	20.12	.97	19.15	421		

DATA

Air Temp. = 66.1 °F; $D/_{\nu}$ = 2060 $\frac{sec}{ft}$

Air Speed = 2.8 cmH_2O

= 70 ft/sec

Re = 144,200

Correction Factor = 1.0267

Re_{corr} = 148,050

Voltage = 39.6 V

Heat Flux = 859 BTU/hr.ft²

Film Temp = 88 °F; $D/_{K}$ = 21.8 $\frac{hr\text{-}°F\text{-}ft^2}{BTU}$

Date: 1-26-74

Time: 1425

Crystal reader: FIELD

Data sheet: COOPER

Cylinder Dia. = .33 ft

Cylinder Area = .59 ft²

Resistance = 12.0

Crystals:

R49 538
545 536
543 534
540 532

θ	CRY.	TEMP (°F)	ΔT	h	h_r	h_c	Nu	F_R	Comments
104	R49R	121.7	55.6	15.45	1.05	14.4	314		CRITICAL FLOW
103	R49B	124.2	58.1	14.78	1.06	13.72	299		CONDITIONS!
108	R49B	124.2	58.1	14.78	1.06	13.72	299		V = 39.6
65	R49B	124.2	58.1	14.78	1.06	13.72	299	.78	COOL SPOT IN
122	R49B	124.2	58.1	14.78	1.06	13.72	299		BOBBLE
115	R49R	121.7	55.6	13.94	1.05	12.89	281		V = 37.6 V
70	R49B	124.2	58.1	13.34	1.06	12.28	268	.7	q = 775
97	R49B	124.2	58.1	13.34	1.06	12.28	268		2nd SEPERATION
		VOLTAGE 29.2, T∞ = 66.4 °F q = 467							POINT
30	S34G	95.2	28.2	16.2	.97	15.23	332	.86	
50	S34B	96.3	29.9	15.62	.98	14.64	319	.83	
65	S36B	99.4	33	14.15	.99	13.16	287	.75	
72	S38B	103.9	37.5	12.45	1.00	11.45	250	.65	
75	S40B	107.1	40.7	11.47	1.01	10.46	228	.59	
77	S43B	112.3	45.9	10.17	1.02	9.15	199	.52	1ST
81	R49R	121.7	55	8.49	1.05	7.44	162		SEPERATION
88	S43B	112.3	45.9	10.17	1.02	9.15	199		
90	S40B	107.1	40.7	11.47	1.01	10.46	228		
97	S38B	103.9	37.5	12.45	1.00	11.46	250		
115	S36B	99.4	33	14.15	.99	13.16	287		
133	S34B	96.3	29.9	15.62	.98	14.60	319		
150	S32B	92.6	26.2	17.82	.96	16.86	368		
	VOLTAGE 32.T, T∞ = 66.5, q = 565								
0	S36G	98.2	31.7	17.82	.99	16.83	369	.96	
28	S36B	99.4	32.9	17.17	.99	16.18	353	.92	
51	S38B	103.9	37.4	15.11	1.00	14.11	308	.8	
157	S34B	96.3	29.8	18.96	.98	17.98	393		
180	S32G	91.6	25.1	22.51	.96	21.55	470		

APPENDIX B

EDGE EFFECTS

In the set of experiments involving the cylinders constructed from Temsheet, the top and bottom edges of the test section were not guarded against heat losses. An analysis was performed and it was found that edge effects did not influence the temperature field beyond a distance of approximately 1/4 inch. The details of the analysis are presented in this appendix.

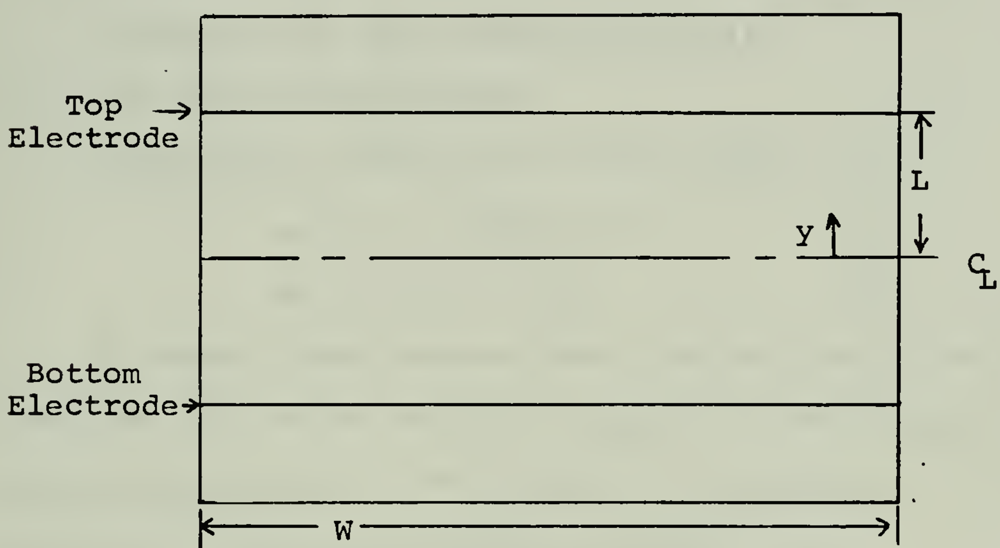

The axial variation in the temperature field due to end losses was estimated by treating the Temsheet as a thin fin. Symmetry about the centerline was assumed. Temperature variations in the circumferential direction were neglected. A "worst case" situation was studied by assuming the temperature at y=L equaled the free stream air temperature, T_∞.

Due to symmetry, the centerline represented an adiabatic surface. The governing equation for this situation is:

$$\frac{dT^2}{dy^2} + \frac{\dot{q}'''}{k} - \frac{h}{kt}(T-T_\infty) = 0 \qquad (1)$$

where

T = Temperature at location y

$\dot{q}'''$ = Volumetric heat generation rate = $V^2/2RLWt$

V = Voltage impressed across the electrodes

R = Electrical resistance of material between electrodes

h = h_c+h_r = Surface heat transfer coefficient

k = Thermal conductivity of test section material

t = Thickness of test section material

T_∞ = Air stream temperature

The boundary conditions on the problem are:

$$\text{at } y = 0,\ dT/dy = 0 \qquad (2)$$

$$\text{at } y = L,\ T = T_\infty \qquad (3)$$

It should also be noted that the surface of the Temsheet that was in contact with the glass wool was assumed to be perfectly insulated. The solution to equation (1) that satisfies boundary conditions (2) and (3) is

$$\frac{T-T_\infty}{T_O-T_\infty} = \left\{1 - \frac{\mathrm{Cosh}(my)}{\mathrm{Cosh}(mL)}\right\} \qquad (4)$$

where

(T_O-T_∞) = Centerline temperature excess = $\frac{\dot{q}'''t}{h}$

$m = \sqrt{\frac{h}{kt}}$

Equation (4) was used to determine the minimum distance from the electrodes that data could be taken and not be

affected to any substantial degree by end losses. As a guideline, equation (4) was used to determine the y location for which $T-T\ /T_O-T_\infty = 0.99$. Using representative values of:

$$2L = 6 \text{ inches}$$

$$h = 5\ \text{BTU/hr-ft}^2\text{-°F}$$

$$k = 0.06\ \text{BTU/hr-ft-°F}$$

$$t = 0.00325\ \text{ft}$$

This distance is found to be:

$$y = 2.78 \text{ inches.}$$

It was concluded that if the electrodes were spaced 6 inches apart, using only the center 4 inches would yield temperature information that was essentially uninfluenced by edge effects. Figure 14 in the body of the Thesis supports this claim.

APPENDIX C

COMPARISON OF THERMOCOUPLES AND LIQUID CRYSTALS

In the set of experiments that employed the Nichrome wrapped cylinder, a comparison was made between the temperature determined with the thermocouples and the temperature as determined visually using the liquid crystal tapes. This comparison was made to serve as a check on the accuracy with which one can determine temperature using liquid crystals. In comparing the two temperature sensing techniques it must be noted that the thermocouples were located on the inside of the Nichrome ribbon whereas the liquid crystals were located on the outside of the tape. As such, a thermal resistance exists between the two locations. This will result in a temperature drop. An elementary heat transfer analysis on the composite system as shown sketched below yields the following expression for this temperature drop

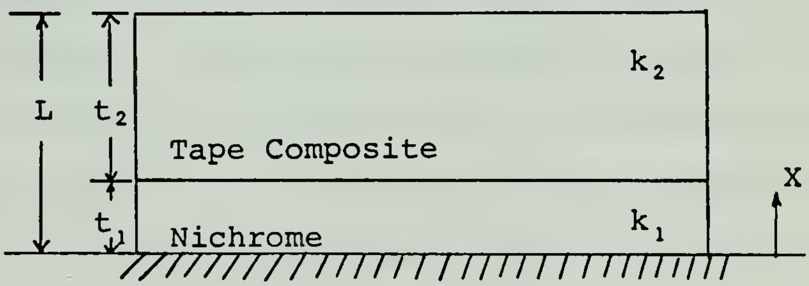

$$\Delta T = \frac{\dot{q}'''L^2}{k_2}\left[\frac{t_1}{L}\left(1-\frac{t_1}{L}\right) + \frac{1}{2}\frac{k_2}{k_1}\left(\frac{t_1}{L}\right)^2\right]$$

The subscripts "1" refers to the Nichrome and the subscript "2" refers to the tape. The volumetric heat

generation term, $\dot{q}'''$, is related to the voltage drop across the ribbon as $\dot{q}''' = V^2/RAt$

where

R = Electrical resistance of the ribbon

A = Total surface area of the ribbon

t = Thickness of the ribbon

V = Voltage

The following were taken as typical thicknesses and properties

t_1 = .00025 ft

t_2 = .00075 ft

k_1 = 5.5 BTU/hr-ft-°F

k_2 = .12 BTU/hr-ft-°F

Using these values the expression for ΔT becomes

$$\Delta T = 2.07 \times 10^{-6}\dot{q}''' \quad [°F]$$

where $\dot{q}'''$ is expressed in BTU/hr-ft^3

The above expression was then used to evaluate the results of the test. Several items where noted. The thermocouple readings should have been higher than those of the liquid crystals. This was not always the case. Careful analysis of the surface showed that the thermocouples were only under tape R-45. The liquid crystal temperature distribution was taken from several tapes. This meant that the temperatures compared were at the same angular location but not necessarily the same vertical location on the cylinder surface.

It should be noted that the location of the thermocouples under tape R-45 was easily found. The thermocouples acted

as a heat sink and could easily be found during warm-up of the cylinder. One showed up as a pin point size cool spot at an angular location of 90°.

Examination of the surface of the cylinder showed that the thermocouple was located on a smooth surface whereas the surface under the tapes directly above or below it could have irregular shape because of the Nichrome ribbon irregularities. The surface irregularities produced hot or cold spots and accounted for the departure from expected results.

Since thermocouple position on tape R-45 was known and the surface there was smooth, it was decided to compare temperature readings at that point. The readings compared within the calculated differences. Table II shows this comparison.

Table II

Comparison of Thermocouple and
Liquid Crystal Temperature Readings

Temperatures (°F)		Temperature Differences (°F)	
Liquid Crystals	Thermocouple	Maximum Predicted	Actual
108.9 (Red)	109.8	2.7	.9
109.9 (Green)	112.5	2.9	2.6
112.1 (Blue)	113.5	3.2	1.4

APPENDIX D

UNCERTAINTY ANALYSIS

The degree of uncertainty for the final results was calculated using the method of Kline and McClintock described in Ref. 20.

The measured variables which were the origins of uncertainty were voltage, resistance, surface temperature, angular location, micromanometer pressure drop, cylinder physical measurements, and the properties of air.

The error in determining the properties of air was negligible.

THE HEAT TRANSFER COEFFICIENT

The heat transfer coefficient was calculated from

$$h = \frac{V^2/R}{A\Delta T}$$

$$\frac{\omega_h}{h} = \sqrt{\left(\frac{2\omega_V}{V}\right)^2 + \left(\frac{\omega_R}{R}\right)^2 + \left(\frac{\omega_{\Delta T}}{\Delta T}\right)^2 + \left(\frac{\omega_A}{A}\right)^2}$$

For the following experimental run at a Reynolds number of 47,818

V	$= 27.6 \pm .3$ VOLTS	(20 to 1)
R	$= 12.0 \pm .3$ OHMS	(20 to 1)
ΔT	$= 39.7 \pm .9°F$	(20 to 1)
A	$= .52 \pm .01$ ft	(20 to 1)

Substituting

$$\frac{\omega_h}{h} = \sqrt{\left(\frac{2\times .3}{27.6}\right)^2 + \left(\frac{.3}{12}\right)^2 + \left(\frac{.9}{39.7}\right)^2 + \left(\frac{.01}{.52}\right)^2}$$

$$\frac{\omega_h}{h} = .045$$

This represents the uncertainty at the forward stagnation without regard to the uncertainty in determining the angular location. It is estimated that the uncertainty in reading angular location in this region would be ±5° (20 to 1).

The uncertainty in the heat transfer coefficient at separation was approximately 4.5 percent with an angular uncertainty of ±1° (20 to 1).

The uncertainty in the wake was on the order of 8 percent with an angular uncertainty of ±5° (20 to 1).

THE NUSSELT NUMBER

The Nusselt number was calculated from the equation

$$Nu = \frac{hD}{K}$$

The uncertainty equation would be

$$\frac{\omega_{Nu}}{Nu} = \sqrt{\left(\frac{\omega_h}{h}\right)^2 + \left(\frac{\omega_D}{D}\right)^2 + \left(\frac{\omega_K}{K}\right)^2}$$

Since the uncertainty in D and K was considered negligible

$$\frac{\omega_{Nu}}{Nu} = \frac{\omega_h}{h}$$

or the same as for heat transfer coefficients.

THE REYNOLDS NUMBER

Reynolds number was calculated from the equation

$$Re = \frac{VD}{\nu}$$

and its uncertainty is the same as free stream velocity, V.

$$V = \sqrt{\frac{2\Delta p}{\rho}}$$

$$\frac{\omega_{Re}}{Re} = \frac{\omega_V}{V} = \sqrt{\left(.5\frac{\omega_{\Delta p}}{\Delta p}\right)^2} = .5\left(\frac{\omega_{\Delta p}}{\Delta p}\right)$$

Since Δp is directly related to manometer reading Δh

$$\frac{\omega_{Re}}{Re} = .5\ \frac{\omega_{\Delta h}}{h}$$

For a Reynolds number of 37,885

$$\frac{\omega_{Re}}{Re} = .5\ \left(\frac{.01}{.19}\right) = .025$$

For a Reynolds number of 148,000

$$\frac{\omega_{Re}}{Re} = .5\ \left(\frac{.01}{2.8}\right) = .002$$

THE FROESSLING NUMBER

The Froessling Number was calculated from $Fr = \frac{Nu}{\sqrt{Re}}$

Then,

$$\frac{\omega_{Fr}}{Fr} = \sqrt{\left(\frac{\omega_{Nu}}{Nu}\right)^2 + \left(\frac{\omega_{Re}}{2Re}\right)^2}$$

Substituting

$$\frac{\omega_{Fr}}{Fr} = \sqrt{(.045)^2 + (.017)^2} = .05$$

This is for the Reynolds number 47,818 used previously. It would decrease with increasing Reynolds numbers.

LIST OF REFERENCES

1. Armed Services Technical Information Agency, AD 66184, "A New Method for Calculating Laminar Heat Transfer on Cylinders of Arbitrary Cross-Section and on Bodies of Revolution at Constant and Variable Wall Temperatures," H. Schuh, 1953.

2. Giedt, W. H., "Investigation of Variation of Point Unit Heat-Transfer Coefficient Around a Cylinder Normal to an Air Stream," Transactions of the ASME, p. 375-381 May 1949.

3. Meyer, J. F., An Experimental Investigation of the Heat Transfer Characteristics of a Heated Cylinder Placed in a Cross Flow of Air, ENGR Thesis, Naval Postgraduate School, 1973.

4. Klein, E. J., "Liquid Crystals in Aerodynamic Testing," Astronautics and Aeronautics, Vol. 6, No. 7, p. 70-73, July 1968.

5. Air Force Flight Dynamics Laboratory, FDMGTM 70-3, Boundary Layer Transition at Supersonic Speeds Measured by Liquid Crystals, by E. D. McElderry, June 1970.

6. Wirzburger, A. H., An Environmental Heat Transfer Study of a Rocket Motor Storage Container System, MSME Thesis, Naval Postgraduate School, 1972.

7. Groff, J. P., Design and Analysis of a Resistively Heated Surgical Probe, MSME Thesis, Naval Postgraduate School, 1971.

8. Petrovic, W. K., An Experimental Investigation of the Temperature Field Produced by a Surgical Cryoprobe, MSME Thesis, Naval Postgraduate School, 1972.

9. Katz, R. G., Experimental Investigation of the Heat Transfer Characteristics of a Radio Frequency Surgical Probe, ENGR Thesis, Naval Postgraduate School, 1973.

10. Groff, J. P. and Cooper, T. E., "Thermal Mapping, via Liquid Crystals, of the Temperature Field near a Heated Surgical Probe," Transactions of the ASME, p. 250-256, May 1973.

11. Petrovic, W. K. and Cooper, T. E., "An Experimental Investigation of the Temperature Field Produced by a Cryosurgical Cannula," paper presented at the Winter Annual Meeting of ASME, Detroit, Michigan, Nov. 11-15, 1973.

12. Katz, R. G. and Cooper, T. E., "Liquid Crystal Display of the Temperature Fields Produced by Radio Frequency Emitting Electrodes," paper presented at 26th ACEMB, Leamington Hotel, Minneapolis, Minn., Sept. 30-Oct. 4, 1973.

13. Fergason, J. L. and Brown, G. H., "Liquid Crystals and Living Systems," Journal of American Oil Chemicals Society, Vol. 45, No. 3, p. 120-127, March 1968.

14. Davis, F., "Liquid Crystals: A New Tool for NDT," Research/Development, p. 24-27, June 1967.

15. Fergason, J. L., "Liquid Crystals," Scientific American, Vol. 211, No. 2, p. 76-86, Aug. 1964.

16. Fergason, J. L., "Liquid Crystals in Non-destructive Testing," Applied Optics, Vol. 7, No. 9, p. 1729-1737, Sept. 1968.

17. Fergason, J. L., "Experiments with Cholesteric Liquid Crystals," Am. J. of Physics, Vol. 38, No. 4, p. 425-428, Apr. 1970.

18. Fage, A. R. C. Sc. and Warsap, J. H., "The Effects of Turbulence and Surface Roughness on the Drag of a Circular Cylinder," Technical Report of the Aeronautical Research Committee, Vol. 1, p. 248-255, Oct. 1929.

19. Lawrence Livermore Laboratory UCRL-73582, Transient Surface Temperature Response of Liquid Crystal Films, by R. Parker, Dec. 14, 1971.

20. Kline, S. J. and McClintock, F. A., "Describing Uncertainties in Single-Sample Experiments," Mech. Engr., Vol. 75, Jan. 1953.

INITIAL DISTRIBUTION LIST

		No. Copies
1.	Defense Documentation Center Cameron Station Alexandria, Virginia 22314	2
2.	Library, Code 0212 Naval Postgraduate School Monterey, California 93940	2
3.	Department Chairman, Code 59 Department of Mechanical Engineering Naval Postgraduate School Monterey, California 93940	1
4.	T. E. Cooper, Code 59cg Department of Mechanical Engineering Naval Postgraduate School Monterey, California 93940	3
5.	W. H. Giedt Department of Mechanical Engineering University of California Davis, California	1
6.	LT R. J. Field USS Shark SSN 591 FPO, New York, N.Y.	1

SECURITY CLASSIFICATION OF THIS PAGE (When Data Entered)

REPORT DOCUMENTATION PAGE		READ INSTRUCTIONS BEFORE COMPLETING FORM
1. REPORT NUMBER	2. GOVT ACCESSION NO.	3. RECIPIENT'S CATALOG NUMBER
4. TITLE (and Subtitle) Liquid Crystal Mapping of the Surface Temperature on a Heated Cylinder Placed in a Crossflow of Air		5. TYPE OF REPORT & PERIOD COVERED Master's Thesis March 1974
		6. PERFORMING ORG. REPORT NUMBER
7. AUTHOR(s) Richard Johns Field		8. CONTRACT OR GRANT NUMBER(s)
9. PERFORMING ORGANIZATION NAME AND ADDRESS Naval Postgraduate School Monterey, California 93940		10. PROGRAM ELEMENT, PROJECT, TASK AREA & WORK UNIT NUMBERS
11. CONTROLLING OFFICE NAME AND ADDRESS Naval Postgraduate School Monterey, California 93940		12. REPORT DATE March 1974
		13. NUMBER OF PAGES 72
14. MONITORING AGENCY NAME & ADDRESS(if different from Controlling Office) Naval Postgraduate School Monterey, California 93940		15. SECURITY CLASS. (of this report) Unclassified
		15a. DECLASSIFICATION/DOWNGRADING SCHEDULE

16. DISTRIBUTION STATEMENT (of this Report)

Approved for public release; distribution unlimited.

17. DISTRIBUTION STATEMENT (of the abstract entered in Block 20, if different from Report)

18. SUPPLEMENTARY NOTES

19. KEY WORDS (Continue on reverse side if necessary and identify by block number)

Liquid Crystals, Forced Convection Heat Transfer, Right circular cylinder heat transfer, Constant heat flux cylinder heat transfer, Bluff body heat transfer, Incompressible flow around a cylinder, Free Stream Turbulence

20. ABSTRACT (Continue on reverse side if necessary and identify by block number)

A liquid crystal thermographic technique has been developed which provides an excellent means of obtaining both qualitative and quantitative heat transfer information on heated objects placed in forced convection environments.

Circumferential variation of the Nusselt number on a uniformly heated right circular cylinder cooled by forced convection was obtained for Reynolds numbers varying from 38,000 to 148,000.

DD FORM 1 JAN 73 1473 EDITION OF 1 NOV 65 IS OBSOLETE
(Page 1) S/N 0102-014-6601

SECURITY CLASSIFICATION OF THIS PAGE (When Data Entered)

Block 20 Abstract (Cont.)

The results compare within the experimental uncertainty in forward stagnation regions with the theory of Schuh. Beyond approximately 30°, the results diverge from theory but are consistent with the work of other investigators.

Block 19 - Key Words (Cont.)

Local heat transfer coefficients around a cylinder, Subcritical Flow around a cylinder, Critical flow around a cylinder.

Field

Liquid crystal mapping of the surface temperature on a heated cylinder placed in a crossflow of air.

Thesis
F423
c.1
149208
Field
Liquid crystal mapping of the surface temperature on a heated cylinder placed in a crossflow of air.